concluded that antigens #7 and #17 were annexin VI and vimentin, respectively. Immunoscreening with phages against other spots (#6, #23, #29, and #36) did not give a positive signal. Then, the protein spots successfully identified on 2D-PP and 5 other randomly chosen ones with negative results were subjected to mass spectrometric protein identification. The antigens except for spot #36 were identified by peptide mass fingerprinting analysis. The molecular weights and isoelectric points of the identified proteins are given in Table II. The SOSUI system (http://sosui.proteome.bio.tuat.ac.jp/sosuiframe0.html) was used to predict the hydropathic profiles and the presence of transmembrane helices of the proteins. All of the identified proteins exhibited negative average hydrophobicity values (Table II), and no transmembrane region in these proteins was predicted.

DISCUSSION

We have developed a novel method that facilitates the selection of phage antibodies directly on two-dimensionally separated protein blots. 2D-PP enables us to obtain antibodies against molecules which have been considered to be difficult targets for a conventional method, obviating the purification of antigens in crude biochemical samples or animal immunization. Actually, antibodies specific to the components of the lipid raft fraction were successfully isolated and these phages could be functionally used for immunobiochemical methods such as Western blotting and ELISA. Furthermore, we demonstrated the applicability of these phage antibodies to the immunoscreening of a cDNA expression library, where annexin VI and vimentin were identified as the target antigens in the lipid rafts. It is known that annexin VI acts as a linker between membrane lipids and the cytoskeleton (*30*), and that vimentin is associated with SNAP-23, for instance, it is Triton X-100 insoluble (*31*). Therefore, these molecules can be observed in detergent-insoluble domains or the lipid raft fraction, and the results of our immunoscreening are reasonable.

The phage panning procedures involving nitrocellulose membranes, however, produced a large quantity of background antibodies, such as anti-nitrocellulose phages, and the efficiency, whether specific antibodies were obtained or not, was limited. As listed in Table II, eight positives were obtained on panning against a total 39 spots (20.5%), and there seemed to be some factors affecting the efficiency of 2D-PP.

The efficacy appeared to be unrelated with the spot sizes, molecular weights, isoelectric points or hydropathicity of the antigen proteins (Fig. 2 and Table II). All of the proteins listed in Table II were categorized as cell membrane-attached proteins or the subunits of membrane protein complexes. At present we do not know which specific characteristics of the proteins affect the results of 2D-PP.

On panning by methods [i] and [ii], we encountered the unexpected propagation of anti-nitrocellulose phages. This problem needs to be resolved, since it would affect the efficiency of 2D-PP more seriously than the characters of the antigen molecules. Each phage clone may have a proper rate of propagation through the panning procedures when the nitrocellulose membrane is used as an immobilization matrix of proteins. When antigen-binding clones proliferate with lower rates of propagation than that of background ones, such as anti-nitrocellulose or anti-blocking reagents phages, the number of positives in the polyclonal phage pool becomes lower, as the panning rounds proceed. In this situation, it will be necessary for a substantial number of individual phage clones to be analyzed for successful selection of positive clones. A robot-based technology, such as an antibody array system, has been developed for the screening of a large number of individual clones (*32*), however, it needed a large amount of antigens for selection. Another solution of the anti-nitrocellulose phage problem is to avoid the use of nitrocellulose membranes, as expected. However, our trial of alternate use of nitrocellulose and PVDF was not successful, which was inconsistent with the results of Liu and Marks (*33*). Theoretically, an immobilization matrix that has a high protein binding capacity but low affinity with background phages, and no antigenicity by itself is most suitable for 2D-PP, in particular for targeting the small quantities of antigens. Possibly, the microstructures of the membrane surface also affect the effi-ciency of 2D-PP. We observed that phage antibodies often failed to react with an antigen blot when reprobed after stripping of the antibody complex on the blots, whereas the usual antibody molecules such as IgG showed reproducible reactivity in such reprobing experiments. This was presumably because the antigens near the surface were stripped off during the reprobing procedure, and the phage antibody particles, about 900 × 10 nm in size (*34*), would not have access to the antigen molecules immobilized deep in the pores of the nitrocellulose membrane, although IgG (about 10 nm) could reach them. In this context, an immobilization matrix without pores will be advantageous for protein blotting in 2D-PP, which may be obtained using a new material such as conductive polymers.

In post-genomic bioscience, our 2D-PP will be a strong tool in combination with proteomic analysis performed by 2-D PAGE and mass spectrometry. 2-D PAGE/mass spectrometry is an increasingly used experimental system for the identification of proteins with high sensitivity. However, when specific antibodies are needed for further functional analysis of such identified proteins, each of the target proteins must be individually prepared in a large amount and subjected to laborious animal immunization to generate antibodies. In this context, 2D-PP is highly advantageous, since it can rapidly and directly give us antibodies against each protein separated by 2-D PAGE, even from insoluble crude fractions. Also, "the antibody catalog" can be made when antibodies are selected for each component in some characteristic protein fractions. The antibody set is applicable to the development of therapeutics or antibody chips useful for diagnosis or protein expression profiling in many diseases.

We are grateful to Dr. G. Winter for providing the Griffin.1 library and critical reading of the manuscript, Drs. M. Nishijima, Y. Yamakawa, and T. Kinumi for the helpful discussion, and Dr. K. Ishida for the useful advice on immunoscreening. We also thank D. Nishikiori for the technical assistance.

REFERENCES

1. Pandey, A. and Mann, M. (2000) Proteomics to study genes and genomes. *Nature* **405**, 837–846
2. Barbas, C.F., Kang, A.S., Lerner, R.A., and Benkovic, S.J. (1991)

Assembly of combinatorial antibody libraries on phage surfaces: the gene III site. *Proc. Natl. Acad. Sci. USA* **88**, 7978–7982
3. Marks, J.D., Hoogenboom, H.R., Bonnert, T.P., McCafferty, J., Griffiths, A.D., and Winter, G. (1991) By-passing immunization. Human antibodies from V-gene libraries displayed on phage. *J. Mol. Biol.* **222**, 581–597
4. Burton, D.R. and Barbas, C.F. (1994) Human antibodies from combinatorial libraries. *Adv. Immunol.* **57**, 191–280
5. Hoogenboom, H.R., De Bruine, A.P., Hufton, S.E., Hoet, R.M., Arends, J.W., and Roovers, R.C. (1998) Antibody phage display technology and its applications. *Immunotechnology* **4**, 1–20
6. Griffiths, A.D., Malmqvist, M., Marks, J.D., Bye, J.M., Embleton, M.J., McCafferty, J., Baier, M., Holliger, K.P., Gorick, B.D., Hughes-Jones, N.C., Hoogenboom, H.R., and Winter, G. (1993) Human anti-self antibodies with high specificity from phage display libraries. *EMBO J.* **12**, 725–734
7. Griffiths, A.D., Williams, S.C., Hartley, O., Tomlinson, I.M., Waterhouse, P., Crosby, W.L., Kontermann, R.E., Jones, P.T., Low, N.M., Allison, T.J., Prospero, T.D., Hoogenboom, H.R., Nissim, A., Cox, J.P.L., Harrison, J.L., Zaccolo, M., Gherardi, E., and Winter, G. (1994) Isolation of high affinity human antibodies directly from large synthetic repertoires. *EMBO J.* **13**, 3245–3260
8. Marks, J.D., Ouwehand, W.H., Bye, J.M., Finnern, R., Gorick, B.D., Voak, D., Thorpe, S.J., Hughes-Jones, N.C., and Winter, G. (1993) Human antibody fragments specific for human blood group antigens from a phage display library. *Biotechnology* **11**, 1145–1149
9. Siegel, D.L. and Silberstein, L.E. (1994) Expression and characterization of recombinant anti-Rh(D) antibodies on filamentous phage: a model system for isolating human red blood cell antibodies by repertoire cloning. *Blood* **83**, 2334–2344
10. De Kruif, J., Terstappen, L., Boel, E., and Logtenberg, T. (1995) Rapid selection of cell subpopulation-specific human monoclonal antibodies from a synthetic phage antibody library. *Proc. Natl. Acad. Sci. USA* **92**, 3938–3942
11. Noronha, E.J., Wang, X., Desai, S.A., Kageshita, T., and Ferrone, S. (1998) Limited diversity of human scFv fragments isolated by panning a synthetic phage-display scFv library with cultured human melanoma cells. *J. Immunol.* **161**, 2968–2976
12. Hoogenboom, H.R., Lutgerink, J.T., Pelsers, M.M., Rousch, M.J., Coote, J., Van Neer, N., De Bruine, A., Van Nieuwenhoven, F.A., Glatz, J.F., and Arends, J.W. (1999) Selection-dominant and nonaccessible epitopes on cell-surface receptors revealed by cell-panning with a large phage antibody library. *Eur. J. Biochem.* **260**, 774–784
13. Masserini, M., Palestini, P., and Pitto, M. (1999) Glycolipid-enriched caveolae and caveolae-like domains in the nervous system. *J. Neurochem.* **73**, 1–11
14. Zhou, J.N., Linder, S., Franzen, B., Auer, G., Hochstrasser, D.F., and Persson, M.A. (1998) Rapid isolation of phage displayed antibodies to β-actin eluted from two-dimensional electrophoresis gel. *Electrophoresis* **19**, 1808–1810
15. Pini, A., Viti, F., Santucci, A., Carnemolla, B., Zardi, L., Neri, P., and Neri, D. (1998) Design and use of a phage display library. Human antibodies with subnanomolar affinity against a marker of angiogenesis eluted from a two-dimensional gel. *J. Biol. Chem.* **273**, 21769–21776
16. Lisanti, M.P., Scherer, P.E., Vidugiriene, J., Tang, Z., Hermanowski-Vosatka, A., Tu, Y.H., Cook, R.F., and Sargiacomo, M. (1994) Characterization of caveolin-rich membrane domains isolated from an endothelial-rich source: implications for human disease. *J. Cell Biol.* **126**, 111–126
17. Sambrook, J. and Russell, D.W. (2001) *Molecular Cloning. A Laboratory Manual*, Cold Spring Harbor Laboratory Press, Cold Spring Harbor, NY
18. Van Dam, A.P., Van den Brink, H.G., and Smeenk, R.J.T. (1990) Technical problems concerning the use of immunoblots for the detection of antinuclear antibodies. *J. Immunol. Methods* **129**, 63–70
19. Saiki, R.K., Gelfand, D.H., Stoffel, S., Scharf, S.J., Higuchi, R., Horn, G.T., Mullis, K.B., and Erlich, H.A. (1988) Primer-directed enzymatic amplification of DNA with a thermostable DNA polymerase. *Science* **239**, 487–491
20. Shevchenko, A., Wilm, M., Vorm, O., and Mann, M. (1996) Mass spectrometric sequencing of proteins silver-stained polyacrylamide gels. *Anal. Chem.* **68**, 850–858
21. Lahm, H.W. and Langen, H. (2000) Mass spectrometry: a tool for the identification of proteins separated by gels. *Electrophoresis* **21**, 2105–2114
22. Simons, K. and Ikonen, E. (1997) Functional rafts in cell membranes. *Nature* **387**, 569–572
23. Brown, D.A. and London, E. (2000) Structure and function of sphingolipid- and cholesterol-rich membrane rafts. *J. Biol. Chem.* **275**, 17221–17224
24. Simons, K. and Ikonen, E. (2000) How cells handle cholesterol. *Science* **290**, 1721–1726
25. Ravn, P., Kjaer, S., Jensen, K.H., Wind, T., Jensen, K.B., Kristensen, P., Brosh, R.M., Orren, D.K., Bohr, V.A., and Clark, B.F. (2000) Identification of phage antibodies toward the Werner protein by selection on Western blots. *Electrophoresis* **21**, 509–516
26. Rohringer, R. and Holden, D.W. (1985) Protein blotting: detection of proteins with colloidal gold, and of glycoproteins and lectins with biotin-conjugated and enzyme probes. *Anal. Biochem.* **144**, 118–127
27. Egger, D. and Bienz, K. (1987) Colloidal gold staining and immunoprobing of proteins on the same nitrocellulose blot. *Anal. Biochem.* **166**, 413–417
28. Schapira, A.H.V. and Keir, G. (1988) Two-dimensional protein mapping by gold stain and immunoblotting. *Anal. Biochem.* **169**, 167–171
29. Altschul, S.F., Gish, W., Miller, W., Myers, E.W., and Lipman, D.J. (1990) Basic local alignment search tool. *J. Mol. Biol.* **215**, 403–410
30. Babiychuk, E.B. and Draeger, A. (2000) Annexins in cell membrane dynamics. Ca^{2+}-regulated association of lipid microdomains. *J. Cell Biol.* **150**, 1113–1123
31. Faigle, W., Colucci-Guyon, E., Louvard, D., Amigorena, S., and Galli, T. (2000) Vimentin filaments in fibroblasts are a reservoir for SNAP23, a component of the membrane fusion machinery. *Mol. Biol. Cell* **11**, 3485–3494
32. De Wildt, R.M.T., Mundy, C.R., Gorick, B.D., and Tomlinson, I.M. (2000) Antibody arrays for high-throughput screening of antibody-antigen interactions. *Nat. Biotechnol.* **18**, 989–994
33. Liu, B. and Marks, J.D. (2000) Applying phage antibodies to proteomics: selecting single chain Fv antibodies to antigens blotted on nitrocellulose. *Anal. Biochem.* **286**, 119–128
34. Day, L.A., Marzec, C.J., Reisberg, S.A., and Casadevall, A. (1988) DNA packing in filamentous bacteriophages. *Annu. Rev. Biophys. Biophys. Chem.* **17**, 509–539

Microglia–Müller Glia Cell Interactions Control Neurotrophic Factor Production during Light-Induced Retinal Degeneration

Takayuki Harada,[1,3,4,6*] Chikako Harada,[1,3,4,6*] Shinichi Kohsaka,[2] Etsuko Wada,[1] Kazuhiko Yoshida,[3] Shigeaki Ohno,[3] Hiroshi Mamada,[4] Kohichi Tanaka,[4,5] Luis F. Parada,[6] and Keiji Wada[1]

Departments of [1]Degenerative Neurological Diseases and [2]Neurochemistry, National Institute of Neuroscience, National Center of Neurology and Psychiatry, Kodaira, Tokyo 187-8502, Japan, [3]Department of Ophthalmology and Visual Sciences, Hokkaido University Graduate School of Medicine, Sapporo, Hokkaido 060-8638, Japan, [4]Department of Molecular Neuroscience, Medical Research Institute, Tokyo Medical and Dental University, Tokyo 113-8510, Japan, [5]PRESTO, Japan Science and Technology Corporation, Kawaguchi, Saitama 332-0012, Japan, and [6]Center for Developmental Biology and Kent Waldrep Foundation Center for Basic Research on Nerve Growth and Regeneration, University of Texas Southwestern Medical Center, Dallas, Texas 75390-9133

Activation of microglia commonly occurs in response to a wide variety of pathological stimuli including trauma, axotomy, ischemia, and degeneration in the CNS. In the retina, prolonged or high-intensity exposure to visible light leads to photoreceptor cell apoptosis. In such a light-reared retina, we found that activated microglia invade the degenerating photoreceptor layer and alter expression of neurotrophic factors such as nerve growth factor (NGF), ciliary neurotrophic factor (CNTF), and glial cell line-derived neurotrophic factor (GDNF). Because these neurotrophic factors modulate secondary trophic factor expression in Müller glial cells, microglia–Müller glia cell interaction may contribute to protection of photoreceptors or increase photoreceptor apoptosis. In the present study, we demonstrate the possibility that such functional glia–glia interactions constitute the key mechanism by which microglia-derived NGF, brain-derived neurotrophic factor (BDNF), and CNTF indirectly influence photoreceptor survival, although the receptors for these neurotrophic factors are absent from photoreceptors, by modulating basic fibroblast growth factor (bFGF) and GDNF production and release from Müller glia. These observations suggest that microglia regulate the microglia–Müller glia–photoreceptor network that serves as a trophic factor-controlling system during retinal degeneration.

Key words: microglia; Müller glial cell; photoreceptor; neurotrophins; glia–glia interaction; glia–neuron interaction; retinal degeneration

Many growth factors and neurotrophins have been shown to promote the survival of retinal neurons. For example, intraocular injection of brain-derived neurotrophic factor (BDNF), neurotrophin-3 (NT-3), ciliary neurotrophic factor (CNTF), glial cell line-derived neurotrophic factor (GDNF), or basic fibroblast growth factor (bFGF) rescues photoreceptors in animal models of retinal degeneration (Faktorovich et al., 1990, 1992; LaVail et al., 1992, 1998; Cayouette et al., 1998; Chong et al., 1999; Frasson et al., 1999). BDNF and NT-3 mediate cell survival via two types of transmembrane glycoproteins, the high-affinity trk tyrosine kinase receptors and the low-affinity neurotrophin receptor p75 ($p75^{NTR}$) (Barbacid, 1994). On the other hand, signal transduction by CNTF requires that it bind first to CNTFRα, a receptor anchored to the cell membrane through a glycosyl-phosphatidylinositol (GPI) linkage (Ip et al., 1993). The binding of CNTF to CNTFRα leads to recruitment and dimerization of gp130 and leukemia inhibitory factor receptor (Davis et al., 1993). GDNF and neurturin act through multicomponent receptor complexes, namely the ligand-binding GPI-linked proteins (GFRα1 and GFRα2) and the transmembrane protein tyrosine kinase Ret (Baloh et al., 2000; Harada et al., 2002).

Paradoxically, BDNF and CNTF are consistently reported as neuroprotective for photoreceptor cells, although these cells do not express their receptors (Ugolini et al., 1995; Kirsch et al., 1997; Harada et al., 2000). However, intraocular administration of BDNF or CNTF activates Müller glial cells exclusively (not photoreceptors) (Wahlin et al., 2000). In addition, BDNF has no direct effect on isolated photoreceptor cells (Carwile et al., 1998). Thus, these trophic factors may protect photoreceptors, at least partly, through Müller glial cells (Zack, 2000; Bringmann and Reichenbach, 2001). In fact, Müller cells contain receptors for most of the molecules involved in photoreceptor rescue and become stimulated after retinal insults such as mechanical injury (Harada et al., 1995; Wen et al., 1995; Yoshida et al., 1995), ischemia (Ju et al., 1999), and light-induced degeneration (Wen et al., 1998). We previously provided additional direct support for such a "Müller cell hypothesis" in that Müller cells, acting in response to NT-3 or nerve growth factor (NGF), respectively, increase or decrease their production of bFGF, which in turn results in either the protection or increased apoptosis of photoreceptor cells (Harada et al., 2000). However, the origin of endogenous trophic factors with which Müller cells interact during photoreceptor degeneration remains unclear.

Received Jan. 11, 2002; revised Aug. 5, 2002; accepted Aug. 7, 2002.

This work was supported in part by grants from the Ministry of Health, Labour and Welfare of Japan, and the Ministry of Education, Culture, Sports, Science and Technology of Japan. T.H. was supported by a Human Frontier Science Program long-term fellowship (LT00170/2001-B), and C.H. was supported by a Uehara Memorial Foundation postdoctoral fellowship. We thank M. Watanabe for providing the antibody to GLAST and L. F. Reichardt for providing the antibody to $p75^{NTR}$.

*T.H. and C.H. contributed equally to this work.

Correspondence should be addressed to Dr. Takayuki Harada, Department of Molecular Neuroscience, Medical Research Institute, Tokyo Medical and Dental University, 1-5-45 Yushima, Bunkyo-ku, Tokyo 113-8510, Japan. E-mail: harada.aud@mri.tmd.ac.jp.

Inherited retinal degeneration is accompanied by the migration of phagocytic cells into the outer retina where photoreceptor degeneration occurs, and the phagocytic cells are derived from resident microglial cells and not from peripheral macrophages (Thanos, 1992; Roque et al., 1996). These results suggest that microglial cells play a critical role during photoreceptor degeneration. However, it is still unknown whether microglia contribute to the neuroprotection by producing neurotrophic factors or exert a cytotoxic function by releasing reactive oxygen species, nitric oxide, or inflammatory cytokines (Kreutzberg, 1996; Graeber et al., 1998; Ito et al., 1998, 2001; Nakajima et al., 1998, 2001). In the present study, we examine the effect of photoreceptor degeneration on the production of neurotrophic factors in microglia and propose a possible mechanism for communication between microglia and neighboring Müller glia and photoreceptors. We also examine whether the Müller cell hypothesis holds for BDNF, CNTF, and GDNF, as it does for NGF and NT-3 (Harada et al., 2000).

MATERIALS AND METHODS

Experimental animals. Experiments were performed using Wistar rats, C57BL/6J mice, and $p75^{NTR}$ knock-out mice (purchased from the Jackson Laboratory) in accordance with the ARVO statement for the Use of Animals in Vision Research. Animals were maintained in either a 12 hr light/dark cycle (LD 12:12) or 24 hr of constant illumination. Light intensity inside the cages ranged from 100 to 200 lux under LD 12:12, whereas 800–1300 lux was used for 24 hr of constant illumination to effect light-induced retinal degeneration (Harada et al., 1996, 1998a).

Immunohistochemistry. Rats were anesthetized with diethylether and perfused transcardially with saline, followed by 4% paraformaldehyde in 0.1 M phosphate buffer containing 0.5% picric acid at room temperature. Rat eyes were removed and postfixed overnight in the same fixative and then embedded in paraffin. The posterior portion of the eye was sectioned sagittally at 7 μm thickness, mounted, and stained with hematoxylin and eosin. For immunohistochemical staining, the sections were incubated in PBS containing 10% normal goat serum for 30 min at room temperature. They were then incubated overnight with a microglia-specific rabbit polyclonal antibody, iba1 (1.0 μg/ml) (Graeber et al., 1998; Ito et al., 1998, 2001; Nakajima et al., 1998) and a mouse monoclonal antibody against ED1 (Serotec; 100×) and visualized with Cy3-conjugated goat anti-rabbit IgG (Amersham Biosciences) and FITC-conjugated goat anti-mouse IgG (Jackson ImmunoResearch). The sections were examined with a confocal laser scanning microscope (Olympus).

Cell culture. Microglial cells were isolated from postnatal day (P) 35 rat eyes reared under LD 12:12 or 24 hr of constant illumination and cultured as described previously (Roque and Caldwell, 1993). These culture cells were examined immunocytochemically after incubation with the rabbit polyclonal antibody iba1 (1.0 μg/ml) or a Müller cell-specific antibody against GLAST (1.0 μg/ml) (Harada et al., 1998b). A portion of culture medium was used to quantify NGF (Chemicon), NT-3 (Promega), GDNF (Promega), and bFGF (R & D Systems) protein expression levels using ELISA assay kits.

Müller cells were isolated from P35 rat eyes and cultured according to an established protocol (Hicks and Courtois, 1990). Total RNA for PCR was prepared from these cells that were either unstimulated or stimulated with 100 ng/ml of recombinant BDNF, CNTF, bFGF, or GDNF for 12 hr. In some experiments (see Figs. 4, 5), these Müller culture cells were incubated with microglia-conditioned medium (MCM) for 12 hr. MCM was prepared from both normal and light-damaged retina, and the final medium change was performed 72 hr before use. Trk-specific inhibitor K252a (Kyowa Hakko; 100 ng/ml), NT-3 blocking antibody (Chemicon; 1 μg/ml), and REX antiserum directed toward the extracellular domain of the $p75^{NTR}$ (Weskamp and Reichardt, 1991) (courtesy of L. F. Reichardt, University of California San Francisco) (diluted 1:100) were added 30 min before MCM treatment.

Laser capture microdissection. Laser capture microdissection (LCM) was performed as described (Harada et al., 2000). Fifty frozen sections (7 μm thick) were made from each P35 eye and stained with hematoxylin. LCM system LM200 (Olympus) was used for laser capture. Following the manufacturer's protocols, samples were obtained from the outer nuclear layer (ONL) (see Fig. 3*A*,*B*), avoiding contamination from neighboring layers. Total RNA was extracted from the LCM samples from three independent animals in both the normal and light-reared groups.

Quantitative RT-PCR analysis. Complementary DNA reverse transcribed from total RNA was amplified by using specific primers as shown in the supplemental Table (available at www.jneurosci.org). Negative controls for PCR were performed using "templates" derived from reverse transcription (RT) reactions lacking either reverse transcriptase or total RNA. Quantitative RT-PCR analysis was performed as reported previously (Harada et al., 1998a). To construct a standard curve, 3.75–30 ng of total RNA was reverse transcribed, and the resulting cDNA was subjected to 20 (G3PDH), 38 [NT-3, Ret, and inducible nitric oxide synthase (iNOS)], or 32 (others) cycles of PCR. Ten microliters of each reaction mixture were removed after each cycle during cycles 12–20 (G3PDH), 30–38 (NT-3, Ret, and iNOS) or 24–32 (others) and electrophoresed on a 2% Tris borate-EDTA Agarose gel. The gel was stained with ethidium bromide to detect the bands of amplified fragments, which were quantitated using a CCD image sensor (ChemiImager, Alpha Innotech). To determine the linear range of PCR product accumulation, the results were plotted on a semilogarithmic scale against the PCR cycle number or on a logarithmic scale against the amount of template RNA used in the reverse transcription reaction. On the basis of these results, subsequent RT-PCR analyses were performed using 15 ng total RNA with PCR cycle numbers shown in the supplemental Table (available at www.jneurosci.org). The intensity of the band from each gene was normalized to the intensity of the band from G3PDH. For this purpose, the primers for G3PDH mRNA were added to the reaction mixture after some reactions to make its final PCR cycle number to be 18. This normalized value was used to determine the relative expression level in each gene.

Statistics. Data are presented as mean ± SEM except as noted. When statistical analysis was performed, one-factor ANOVA was used to estimate the significance of the results. Statistical significance was accepted at $p < 0.05$.

RESULTS

Microglial cells migrate to the outer retina during light-induced retinal degeneration

We first examined the distribution of microglial cells in normal and light-degenerated rat retinas at P35. In these experiments, we used a microglia-specific antibody that recognizes iba1, a new member of the EF hand family of proteins that are present on resting as well as activated and phagocytic microglia (Graeber et al., 1998; Ito et al., 1998, 2001; Nakajima et al., 1998). Anti-iba1 recognizes microglial epitopes from a wide variety of species and is suitable for double-labeling experiments in combination with monoclonal markers. In normal retina, iba1 immunoreactivity was observed only in the inner part of the retina, such as the ganglion cell layer (GCL) and the inner nuclear layer (INL) (Fig. 1*A*). These immunostained cells are characteristic of "resting," ramified microglia (Slepko and Levi, 1996). In light-reared retina, photoreceptor degeneration begins after P21, and approximately half of the photoreceptor nuclei disappear by P35 (Fig. 2*A*,*B*) (Harada et al., 1998a). In such light-degenerated retina, iba1 immunoreactivity was observed in the outer as well as inner retina (Fig. 1*D*). Microglial cells in the outer retina appear to change their morphology during retinal degeneration (from having defined processes to a more amorphous/amoeboid shape). Thus, we next examined whether such amoeboid microglial cells are, in fact, "activated" (Slepko and Levi, 1996; Marin-Teva et al., 1998). For this purpose, we used a monoclonal antibody against ED1, an intracellular marker for activated microglia *in vivo* (Graeber et al., 1990). In control retina, all iba1-positive cells were ED1 negative (Fig. 1*C*, *arrows*). However, almost all microglial cells in the outer retina were double-labeled by iba1 and ED1 (Fig. 1*F*, *arrowheads*), although those in the GCL and INL remained ED1 negative (*arrows*) in the light-reared retina.

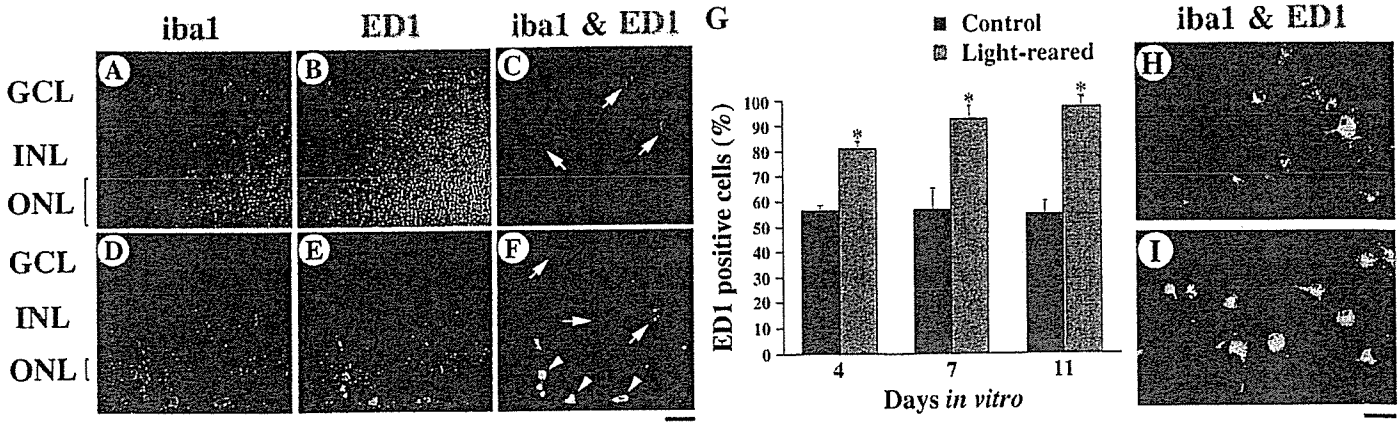

Figure 1. Activation of microglia during light-induced retinal degeneration. *A–F*, Immunohistochemical analysis of normal (*A–C*) and light-reared (*D–F*) P35 rat retina using the antibodies iba1 (*red* in *A*, *C*, *D*, *F*) and ED1 (*green* in *B*, *C*, *E*, *F*). In light-degenerated retina, iba1 immunoreactivity was observed in the outer retina and double-labeled with ED1 (*yellow*) (*F*, *arrowheads*). *G*, Quantitative analysis of the ED1-positive cultured microglial cells from normal (*red bar*) and light-reared (*green bar*) P35 rat retina. Each data point represents the mean ± SEM of the values obtained from six independent experiments; $^*p < 0.05$. *H*, *I*, Double-label immunocytochemistry of cultured microglial cells using the antibodies iba1 (*red*) and ED1 (*green*) from normal (*H*) and light-reared (*I*) P35 rat retina. *GCL*, Ganglion cell layer; *INL*, inner nuclear layer; *ONL*, outer nuclear layer. Scale bars, 30 μm.

Effects of retinal degeneration on the production of trophic factors in microglia

To examine the function of microglia during retinal degeneration, we prepared pure cultured microglial cells from normal and light-degenerated rat retina at P35. In culture, the number of ED1-positive microglia increases with time (Slepko and Levi, 1996). Interestingly, in our culture system the number of ED1-positive microglia (Fig. 1*G*) was greater in cultures from light-reared retina (Fig. 1*I*) than in those from control retina (Fig. 1*H*). In addition, almost all of the cells analyzed were iba1 positive (>99%). Furthermore, by using the Müller cell-specific antibody against GLAST, we determined that Müller glial cell contamination was negligible (data not shown). Using our cultured microglial cells, we examined whether retinal degeneration affects the expression levels of cytotoxic agents produced by these cells. Because nitric oxide produced by microglial cells may injure photoreceptors (Goureau et al., 1994; Cotinet et al., 1997), we examined gene expression of iNOS using quantitative RT-PCR analysis. However, we found that the level of iNOS mRNA in microglia from degenerated retinas was not significantly different from that of normal retinas (Table 1). We next examined the effect of retinal degeneration on microglia with respect to the expression of neurotrophic factors (Shimojo et al., 1991; Frade et al., 1998), which may stimulate photoreceptor survival during retinal degeneration (Faktorovich et al., 1990; LaVail et al., 1992; Cao et al., 1997; Fontaine et al., 1998). RT-PCR indicated that mRNA levels for NGF and NT-3, as well as CNTF and GDNF, were significantly increased in light-reared microglia relative to normal microglia, although this was not the case for BDNF (Table 1). On the other hand, there was an unexpected decrease in bFGF mRNA (Table 1).

In a previous study, we found that exogenous NGF and NT-3 alter bFGF production in Müller glial cells, which act directly on photoreceptor survival (Harada et al., 2000). To determine whether mRNA upregulation of NGF and NT-3 in microglial cells (Table 1) really leads to protein upregulation, we examined protein expression levels in culture medium by ELISA. NGF protein expression level in light-reared culture medium was upregulated to 138 ± 9% ($n = 18$) compared with that in normal culture medium ($p < 0.01$). On the other hand, NT-3 protein expression was below detectable levels in both normal and light-reared culture medium.

We also examined GDNF and bFGF protein expression levels in culture medium. GDNF protein expression level in light-reared culture medium was upregulated to 189 ± 23% ($n = 24$) compared with that in normal culture medium ($p < 0.01$). On the other hand, bFGF protein expression was slightly decreased (93 ± 3%; $n = 18$) ($p < 0.05$). These results are consistent with the data from quantitative RT-PCR analysis (Table 1).

Photoreceptors express receptors for GDNF but not for CNTF in both normal and light-degenerated retina

Because microglial CNTF and GDNF expression is increased during retinal degeneration (Table 1), we examined receptor expression levels in whole retina. In light-reared P35 retina (Fig. 2*B*), the expression of CNTFRα (241 ± 23%; $n = 6$), GFRα1 (140 ± 7%; $n = 6$), and GFRα2 (147 ± 17%; $n = 6$) was significantly upregulated compared with normal retina (Fig. 2*A*) reared under a 12 hr light/dark cycle (Fig. 2*D*,*E*). In addition, gp130 (134 ± 5%; $n = 6$) and LIFRβ (179 ± 15%; $n = 6$) were also upregulated, but this was not the case for Ret (124 ± 5%; $n = 6$) (data not shown). When rats were raised under continuous illumination from P2 to P21, followed by LD 12:12 from P22 to P35, retinal degeneration did not progress after P22 (Fig. 2*C*). Under such conditions, only CNTFRα expression was upregulated (192 ± 26%; $n = 6$) compared with normal retina reared under LD 12:12 (Fig. 2*D*,*E*).

Because our data indicated that CNTF and GDNF receptors are upregulated in light-reared retina, we next determined whether these receptors are localized to photoreceptors. We assayed photoreceptor-specific gene expression of the receptors CNTFRα, GFRα1, and GFRα2 using laser capture microdissection. For this purpose, total RNA was extracted from cells residing in the ONL (Fig. 3*A*,*B*), which is composed of photoreceptor nuclei. However, we were unable to detect CNTFRα gene expression in the ONL (Fig. 3*C*, *lanes 2*, *3*), a result that is consistent with data from previous reports (Ugolini et al., 1995; Kirsch et al., 1997). In contrast, GDNF receptor genes were detected in

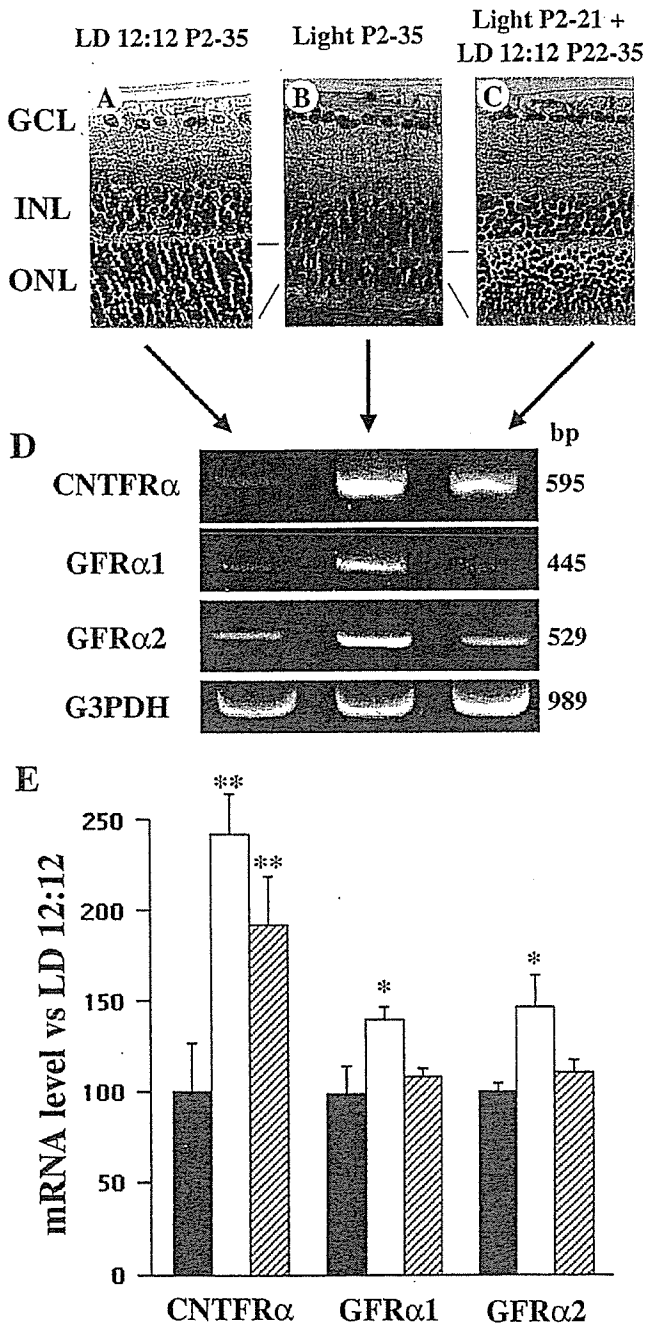

Figure 2. Gene expression of CNTF and GDNF receptors during light-induced retinal degeneration. *A–C*, Light micrograph of retinal sections taken from P35 rats raised under LD 12:12 (*A*), continuous illumination (*B*), or continuous illumination to P21 followed by LD 12:12 from P22 to P35 (*C*). Note the decreased photoreceptor cell number and ONL thickness in *B*. *D*, *E*, Representative data (*D*) and summary (*E*) of quantitative RT-PCR analysis using total RNA extracted from whole retina raised under LD 12:12 (*black bar*), continuous illumination (*white bar*), and continuous illumination to P21 followed by LD 12:12 from P22 to P35 (*hatched bar*). Each data point represents the mean ± SEM of the values obtained from six independent experiments. $^{**}p < 0.01$; $^{*}p < 0.05$. *GCL*, Ganglion cell layer; *INL*, inner nuclear layer; *ONL*, outer nuclear layer.

both normal and light-reared ONL (Fig. 3*C*) (Jing et al., 1996; Jomary et al., 1999). To assess the effect of retinal degeneration on GFRα1/α2 expression, we attempted to quantify expression levels in both normal and light-reared retina, but found that levels were too low for accurate determination. Despite this limitation of our data, these results suggest the possibility that microglia-derived GDNF, but not CNTF, has a direct effect on photoreceptor survival.

Microglia-conditioned medium decreases bFGF production in Müller glial cells

We demonstrated previously that retinal degeneration increases the expression of low-affinity $p75^{NTR}$ in retinal Müller glial cells, resulting in a decrease of bFGF production and photoreceptor apoptosis (Harada et al., 2000). In light of our results that suggest that microglia is a potential source of NGF (Table 1), we next examined the effect of microglia-conditioned medium on bFGF expression in cultured Müller cells (Fig. 4*A*). As shown in Figure 4*F*, light-reared MCM (60 ± 15%; $n = 3$) but not normal MCM (96 ± 14%; $n = 3$) caused a decrease in bFGF mRNA in Müller cells. This decrease was reversed by the addition of a $p75^{NTR}$ neutralizing antibody (111 ± 5%; $n = 3$), but not by a trk receptor-specific blocker (K252a) (37 ± 5%; $n = 3$) (data not shown). These results suggest that $p75^{NTR}$ is involved in the regulation of bFGF expression in Müller cells. To test this hypothesis more definitively, we examined the effect of light-reared MCM on bFGF production in cultured Müller cells from $p75^{NTR}$ knock-out mice (Fig. 5*A*). As shown in Figure 5*B*, although light-reared MCM significantly reduced bFGF expression in cultured Müller cells from control C57BL/6J mice (61 ± 9%; $n = 3$), no effect was observed in Müller cells from $p75^{NTR}$ knock-out mice (109 ± 12%; $n = 3$). These results are consistent with the idea that $p75^{NTR}$ is involved in the control of bFGF production in Müller cells and that a $p75^{NTR}$ ligand (presumably NGF) reduces bFGF production.

Microglia-conditioned medium increases BDNF production in Müller glial cells

We also examined the effect of MCM on the expression of other trophic factors in cultured Müller cells (Fig. 4*A*). Figure 4*C* shows that BDNF mRNA increased in Müller cells when cultured with light-reared MCM (151 ± 18%; $n = 3$) but not normal MCM (82 ± 6%; $n = 3$). However, such was not the case for NGF (Fig. 4*B*), NT-3 (Fig. 4*D*), CNTF (Fig. 4*E*), or GDNF (Fig. 4*G*). Because both trkB and $p75^{NTR}$ are detected in Müller cells (von Bartheld, 1998; Harada et al., 2000), we next examined whether exogenous BDNF may alter the expression of secondary trophic factors in cultured Müller cells (Table 2). After BDNF treatment, both CNTF and bFGF were upregulated. However, given that CNTFRα is absent from photoreceptors (Fig. 3*C*), we further examined the effect of exogenous CNTF on Müller cells after confirming that CNTFRα was expressed in these cells (data not shown). Surprisingly, CNTF treatment upregulated BDNF as well as bFGF expression in Müller cells (Table 2). Because both GFRα1 and GFRα2 genes were expressed in Müller cells (data not shown), we also examined the effect of exogenous GDNF on Müller cells and found increased expression of BDNF, GDNF, and bFGF (Table 2). These results suggest the possibility that microglia-derived CNTF and GDNF may increase BDNF production in Müller cells, resulting, in turn, in bFGF upregulation in other Müller cells. Taken together with the fact that GDNF receptors are expressed in photoreceptors (Fig. 3*C*), microglia-derived GDNF may act through both direct and indirect pathways to rescue photoreceptors during light-induced retinal degeneration.

Table 1. Quantification of mRNA productions in microglial cells

	NGF	BDNF	NT-3	CNTF	bFGF	GDNF	iNOS
Control	101 ± 4	100 ± 5	101 ± 8	100 ± 6	101 ± 5	100 ± 4	100 ± 7
Light reared	131 ± 7*	116 ± 5	294 ± 16*	139 ± 3*	79 ± 4*	140 ± 5*	115 ± 7

mRNA productions were quantified in microglial cells from control and light-reared P35 rat retinas. For each determination, the mRNA production level in controls was normalized to a value of 100. Results of nine independent experiments are presented as the mean ± SEM. *$p < 0.05$ versus control (one-factor ANOVA).

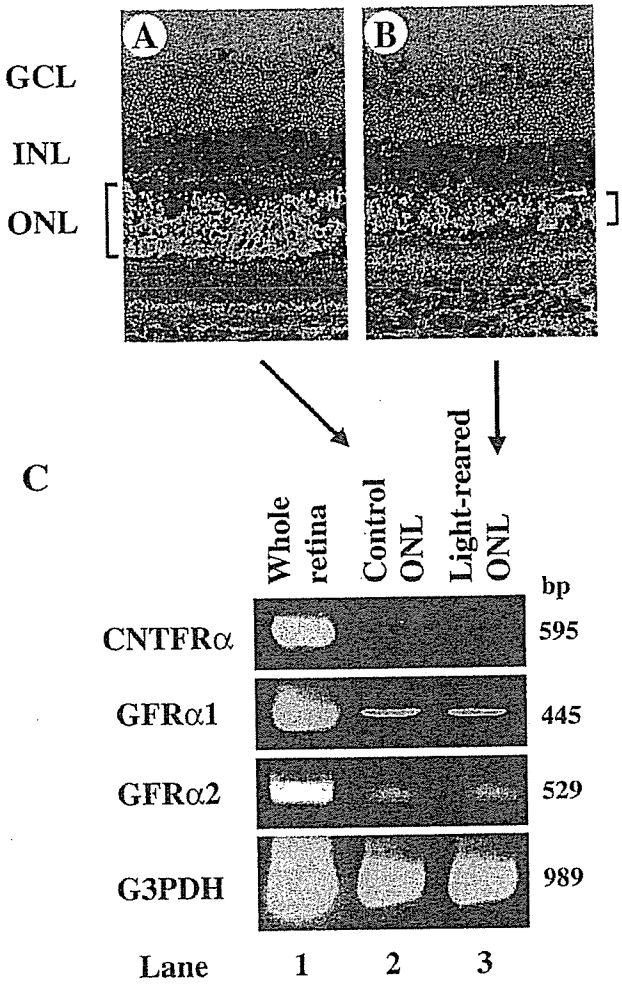

Figure 3. Expression of CNTF and GDNF receptors in P35 rat photoreceptors. *A*, *B*, Cells residing in the ONL were extracted from normal (*A*) and light-reared (*B*) P35 rat retina using a laser-capture microdissection system and then processed for RT-PCR. *C*, RT-PCR analysis of whole retina (*lane 1*) or cells in the ONL from either the control (*lane 2*) or light-reared (*lane 3*) retina. *GCL*, Ganglion cell layer; *INL*, inner nuclear layer; *ONL*, outer nuclear layer.

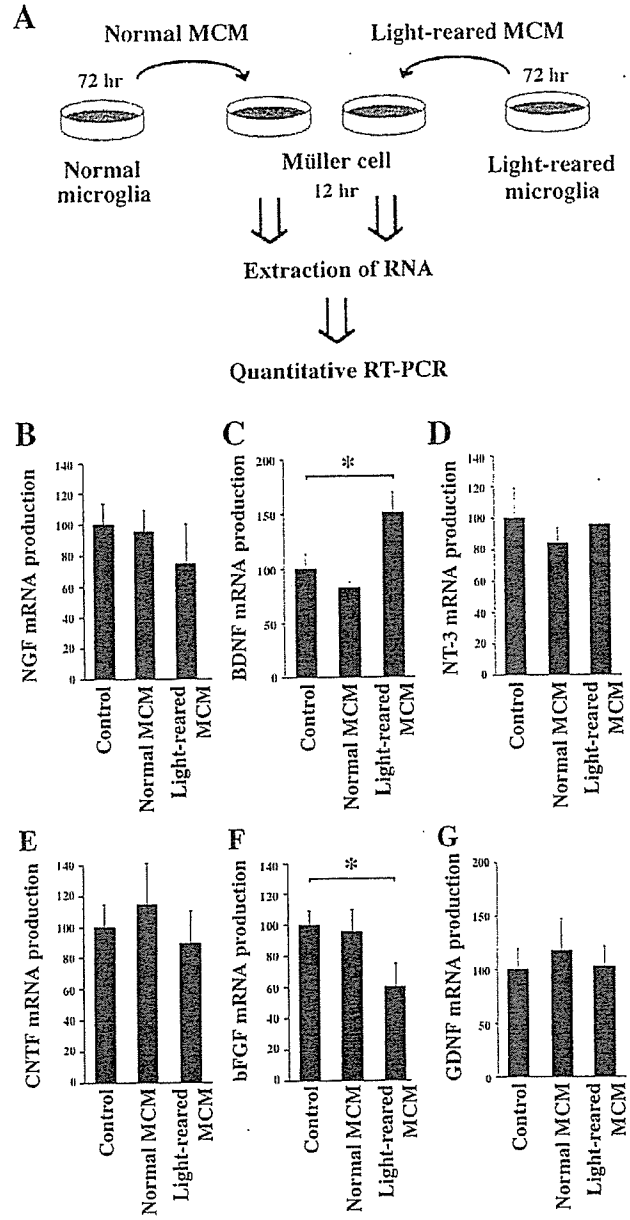

Figure 4. Effect of microglia-conditioned medium (*MCM*) on trophic factor expression in cultured Müller glial cells. *A*, Experimental protocol for examining the effect of MCM prepared from either normal or light-damaged P35 rat retina. Müller cells were incubated with MCM for 12 hr, and mRNA levels of trophic factors were determined by quantitative PT-PCR. *B–G*, RT-PCR analysis of NGF (*B*), BDNF (*C*), NT-3 (*D*), CNTF (*E*), bFGF (*F*), and GDNF (*G*). Note the upregulation of BDNF (*C*) and downregulation of bFGF (*F*) in Müller cells after incubation with light-reared MCM. Each data point represents the mean ± SEM of the values obtained from three independent experiments. *$p < 0.01$.

DISCUSSION

We have shown that retinal degeneration transforms microglia from a resting state to one of "activation." Degenerating photoreceptors influence the migration of microglia from the inner to the outer retina and alter trophic factor production in microglia that may subsequently affect photoreceptor cell survival. Furthermore, microglia-derived factors influence the production of secondary trophic factors in another retinal glial cell type, the Müller cell. As summarized in Figure 6, these findings suggest that functional interactions between microglia and Müller glial cells may be bidirectional and regulate photoreceptor cell survival during retinal degeneration.

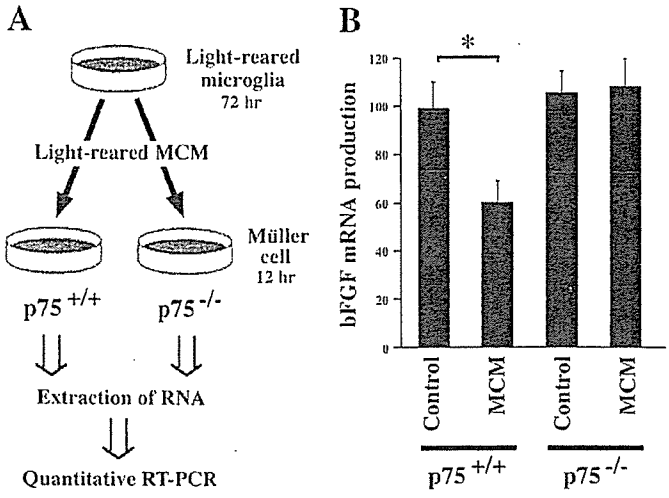

Figure 5. Effect of microglia-conditioned medium (*MCM*) on bFGF expression in cultured Müller cells from $p75^{NTR}$ knock-out mice. *A*, Experimental protocol for examining bFGF mRNA levels in Müller cells from wild-type ($p75^{+/+}$) and $p75^{NTR}$ knock-out ($p75^{-/-}$) mice. Müller cells were incubated with MCM for 12 hr, and bFGF mRNA levels were determined by quantitative RT-PCR. *B*, RT-PCR analysis of bFGF. Note the stable bFGF expression levels in Müller cells from $p75^{NTR}$ knock-out ($p75^{-/-}$) mice. Each data point represents the mean ± SEM of the values obtained from three independent experiments. $^{*}p < 0.01$.

Migration of microglia and microglia-derived factors during retinal degeneration

Prolonged or high-intensity exposure to visible light leads to photoreceptor cell apoptosis (Noell, 1980; Harada et al., 1996, 1998a, 2000; Reme et al., 1998). However, exogenous BDNF, NT-3, CNTF, GDNF, and bFGF can delay this process (Faktorovich et al., 1990, 1992; LaVail et al., 1992, 1998; Cayouette et al., 1998; Chong et al., 1999; Frasson et al., 1999). Our present data suggest that microglia represent a potential endogenous source of these factors (Table 2) and may be available for the protection of photoreceptors. Although microglia increase NGF and GDNF protein productions during retinal degeneration, the opposite is true for bFGF. Similar results have been reported in studies with brain microglia (Araujo and Cotman, 1992). Release of bFGF from brain microglia is reduced by interleukin-3, epidermal growth factor (EGF), and NGF but is slightly augmented by γ-interferon. Together with our present findings, these results suggest that under conditions such as trauma and neurodegeneration, in which there is an imbalance in these molecules, bFGF production in microglial cells may be adversely affected. In addition, the presence of bFGF receptors on photoreceptors (Fontaine et al., 1998) implies that endogenous bFGF release from microglia may serve diverse functions during retinal degeneration. One important point is that the translational products of bFGF mRNA lack a signal peptide sequence that would ordinarily direct its secretion. Although it is not fully understood, many reports conclude that bFGF must somehow escape the cell and indicate mechanisms for bFGF secretion (von Heijne, 1983; Kurokawa et al., 1987; Sato and Rifkin, 1988; Klionsky et al., 1992; Mignatti et al., 1992; Florkiewicz et al., 1995; Piotrowicz et al., 1997; Dow and deVere White, 2000). We have determined previously that the production and secretion of bFGF by Müller cells can be regulated by exogenous NGF and NT-3 (Harada et al., 2000).

In the present study, we also examined NGF and NT-3 protein release from microglia during photoreceptor degeneration. NGF protein expression in culture medium of light-reared microglia was higher than that of normal microglia, but NT-3 protein expression was below detectable levels in both normal and light-reared culture medium. These results are consistent with the data that NGF mRNA expression level was much higher than NT-3. The linear range of PCR product accumulation was 22–26 cycles for NGF (data not shown), so quantification was done at 24 cycles (see supplemental Table available at www.jneurosci.org). On the other hand, it was 32–35 cycles for NT-3 (data not shown), and we needed 33 cycles for quantification (see supplemental Table available at www.jneurosci.org). These results suggest that our quantitative RT-PCR method is truly sensitive to small changes in mRNA levels (e.g., ~30% increase in NGF mRNA lead to ~40% increase in NGF protein), but NT-3 mRNA upregulation did not translate into increased release of NT-3 protein from microglial cells *in vitro*. Because we measured only released NT-3 protein in culture medium, NT-3 protein production in microglia might be upregulated during photoreceptor degeneration, but not released. Another possibility is that released NT-3 might have been consumed by an autocrine mechanism.

The microglia–Müller glia network as a trophic factor regulator during retinal degeneration

We demonstrated previously that trkC and $p75^{NTR}$ are upregulated in Müller cells during retinal degeneration and that exogenous NT-3 increases bFGF production in Müller cells by activating trkC, whereas exogenous NGF decreases bFGF production by activating $p75^{NTR}$ (Harada et al., 2000). In this context, microglia-derived NT-3 and NGF appear to function in opposition to each other. However, the concentration of microglia-released NGF is much higher than that of NT-3, and light-reared MCM decreases bFGF expression in cultured Müller cells (Fig. 4*F*). In addition, light-reared MCM had no effect on cultured Müller cells taken from $p75^{NTR}$ knock-out mice (Fig. 5). These results suggest that the NGF pathway predominates over the NT-3 pathway during retinal degeneration *in vivo*. Frade et al. (1996) demonstrated previously that NGF causes retinal apoptosis during development by activating $p75^{NTR}$. Subsequently, these workers identified microglia as the source of apoptotic NGF in the developing chick retina (Frade and Barde, 1998). Together with our present findings, these results suggest that activated microglia may also be the source of apoptotic NGF in the degenerating adult retina (Fig. 6).

BDNF and CNTF may stimulate photoreceptor survival via the microglia-Müller glia network (Fig. 6) because their appropriate receptors are absent from photoreceptors (Fig. 3). In addition, microglia-derived GDNF may participate in both direct and indirect pathways for photoreceptor rescue. Interestingly, Müller cells treated with GDNF exhibit increased expression of BDNF, bFGF, and GDNF (Table 2). Although enhanced expression of GDNF in response to GDNF treatment may seem odd, a similar observation was reported for bFGF (Cao et al., 1997). We also found that exogenous bFGF upregulates bFGF mRNA (207 ± 16%; $n = 6$) in Müller cells (data not shown). Furthermore, in Müller cells, BDNF treatment increases CNTF expression, and vice versa (Table 2). Because the binding of BDNF, CNTF, and GDNF to their receptors results in tyrosine phosphorylation of cellular substrates, microglia–Müller glia cell interactions may work as a regulator for these trophic factors by using both paracrine and autocrine systems (Fig. 6).

One important issue is the sensitivity of LCM in detecting

Table 2. Quantification of mRNA productions in Müller glial cells

	Control	BDNF treated	CNTF treated	GDNF treated
NGF	100 ± 2	120 ± 7	83 ± 8	82 ± 5
BDNF	101 ± 5	102 ± 7	260 ± 4*	127 ± 4*
NT-3	101 ± 6	95 ± 8	117 ± 10	89 ± 5
CNTF	100 ± 3	149 ± 7*	98 ± 5	110 ± 7
bFGF	101 ± 4	129 ± 4*	162 ± 12*	153 ± 5*
GDNF	100 ± 5	108 ± 6	98 ± 4	145 ± 6*

mRNA productions were quantified in control, BDNF-, CNTF-, and GDNF-treated rat Müller glial cells. For each determination, the mRNA production level in controls was normalized to a value of 100. Results of nine independent experiments are presented as the mean ± SEM. *$p < 0.05$ versus control (one-factor ANOVA).

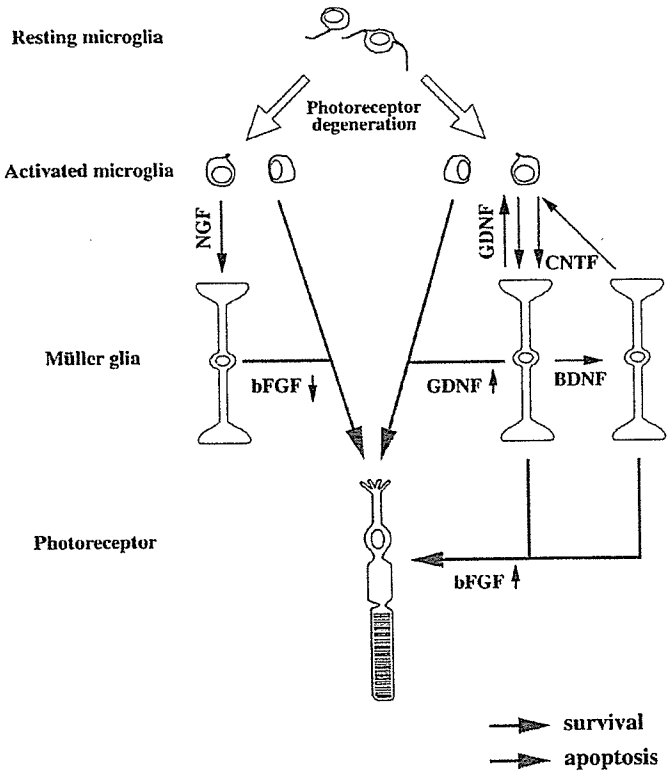

Figure 6. Model for the microglia–Müller glia network in light-degenerated retina. Microglial cells constitutively release various agents that may affect surrounding retinal cells. In light-degenerated retina, reduced bFGF may induce photoreceptor apoptosis, but increased GDNF may directly rescue photoreceptors (*middle*). Microglia-derived GDNF and CNTF increase BDNF and bFGF, whereas BDNF increases CNTF and bFGF production in Müller cells, which may enhance photoreceptor rescue (*right*). On the other hand, microglia-derived NGF reduces bFGF production in Müller cells, which in turn may induce photoreceptor apoptosis (*left*).

photoreceptor-specific trophic factor receptor mRNAs (Fig. 3). Although a recent study demonstrated trkB protein in cone photoreceptors (Di Polo et al., 2000), we could not identify trkB mRNA in photoreceptors isolated by LCM (Harada et al., 2000). This suggests the possibility that our method is insufficient to identify trkB mRNA in cone photoreceptors. In this regard, we note that previous reports were also unable to demonstrate trkB mRNA in photoreceptors by *in situ* hybridization (Jelsma et al., 1993; Perez and Caminos, 1995; Gao et al., 1997; Suzuki et al., 1998; Rohrer et al., 1999). Rohrer et al. (1999) recently demonstrated that signaling paths between trkB-expressing retinal cells (ganglion, amacrine, horizontal, retinal pigment epithelium, and Müller glial cells) and the photoreceptors are required for normal photoreceptor development because photoreceptors do not normally express trkB receptors. Although we have to consider the possibility that photoreceptors may express low levels of trkB and CNTFRα proteins, these results still support the importance of the glia–neuron network in the retina.

Glia–glia and glia–neuron networks as a new therapeutic target for neurodegeneration

Activated microglial cells are observed in various pathological conditions caused by trauma and ischemia and are also involved in pathophysiologies of the CNS, including Alzheimer's disease and AIDS (Kreutzberg, 1996; McGeer and McGeer, 1998; Stoll and Jander, 1999; Le et al., 2001; Nakajima and Kohsaka, 2001). Migration of microglia is thought to be regulated by various factors such as extracellular pH (Faff and Nolte, 2000), nitric oxide (Chen et al., 2000), hepatocyte growth factor (Badie et al., 1999), EGF (Nolte et al., 1997), chemokines (Asensio et al., 1999; Cross and Woodroofe, 1999; Hesselgesser and Horuk, 1999; Maciejewski-Lenoir et al., 1999), and NMDA-induced degeneration (Heppner et al., 1998) to name a few. Thus, by controlling these factors through intervention, microglial migration may be suppressed to an extent sufficient to prevent neural cell apoptosis in various neurological diseases. However, at the same time, such strategies may inhibit the direct neuroprotective effect by microglia-derived factors. Thus it is clear that further investigation is necessary to reveal the functional importance of microglial migration during neurodegeneration.

Our present results suggest that although degeneration is a multicellular and multifactorial process, the functional glia–glia network may provide a new therapeutic target for the treatment of neurodegeneration. The primary function of neurotrophic factors is sustaining the viability of neurons, a process that is counterbalanced by a receptor mechanism that eliminates cells by apoptosis. Such bidirectional control may be used selectively during development and neurodegenerative diseases (Yano and Chao, 2000). Thus, treatment strategies that reinforce survival pathways (Fig. 6, *blue arrows*) or weaken apoptotic pathways (Fig. 6, *red arrows*) may be useful for the prevention of neurodegenerative diseases. Because apoptotic cell death is the final common pathway for photoreceptors in all animal models of retinitis pigmentosa and light-induced retinal degeneration (Steele and O'Tousa, 1990; Chang et al., 1993; Portera-Cailliau et al., 1994; Papermaster and Windle, 1995; Reme et al., 1998; Travis, 1998; Alloway et al., 2000; Harada et al., 2000; Kiselev et al., 2000), the present results raise intriguing possibilities for the management of these pathological conditions by controlling the activity of the microglia–Müller glia–photoreceptor network.

REFERENCES

Alloway PG, Howard L, Dolph PJ (2000) The formation of stable rhodopsin-arrestin complexes induces apoptosis and photoreceptor cell degeneration. Neuron 28:129–138.

Araujo DM, Cotman CW (1992) Basic FGF in astroglial, microglial, and neuronal cultures: characterization of binding sites and modulation of release by lymphokines and trophic factors. J Neurosci 12:1668–1678.

Asensio VC, Lassmann S, Pagenstecher A, Steffensen SC, Henriksen SJ, Campbell IL (1999) C10 is a novel chemokine expressed in experimental inflammatory demyelinating disorders that promotes recruitment of macrophages to the central nervous system. Am J Pathol 154:1181–1191.

Badie B, Schartner J, Klaver J, Vorpahl J (1999) In vitro modulation of microglia motility by glioma cells is mediated by hepatocyte growth factor/scatter factor. Neurosurgery 44:1077–1083.

Baloh RH, Enomoto H, Johnson Jr EM, Milbrandt J (2000) The GDNF family ligands and receptors—implications for neural development. Curr Opin Neurobiol 10:103–110.

Barbacid M (1994) The Trk family of neurotrophin receptors. J Neurobiol 25:1386–1403.

Bringmann A, Reichenbach A (2001) Role of Müller cells in retinal degenerations. Front Biosci 6:E72–92.

Cao W, Wen R, Li F, Cheng T, Steinberg RH (1997) Induction of basic fibroblast growth factor mRNA by basic fibroblast growth factor in Müller cells. Invest Ophthalmol Vis Sci 38:1358–1366.

Carwile ME, Culbert RB, Sturdivant RL, Kraft TW (1998) Rod outer segment maintenance is enhanced in the presence of bFGF, CNTF and GDNF. Exp Eye Res 66:791–805.

Cayouette M, Behn D, Sendtner M, Lachapelle P, Gravel C (1998) Intraocular gene transfer of ciliary neurotrophic factor prevents death and increases responsiveness of rod photoreceptors in the retinal degeneration slow mouse. J Neurosci 18:9282–9293.

Chang G-Q, Hao Y, Wong F (1993) Apoptosis: final common pathway of photoreceptor death in *rd*, rds, and rhodopsin mutant mice. Neuron 11:595–605.

Chen A, Kumar SM, Sahley CL, Muller KJ (2000) Nitric oxide influences injury-induced microglial migration and accumulation in the leech CNS. J Neurosci 20:1036–1043.

Chong NH, Alexander RA, Waters L, Barnett KC, Bird AC, Luthert PJ (1999) Repeated injections of a ciliary neurotrophic factor analogue leading to long-term photoreceptor survival in hereditary retinal degeneration. Invest Ophthalmol Vis Sci 40:1298–1305.

Cotinet A, Goureau O, Hicks D, Thillaye-Goldenberg B, de Kozak Y (1997) Tumor necrosis factor and nitric oxide production by retinal Müller glial cells from rats exhibiting inherited retinal dystrophy. Glia 20:59–69.

Cross AK, Woodroofe MN (1999) Chemokines induce migration and changes in actin polymerization in adult rat brain microglia and a human fetal microglial cell line in vitro. J Neurosci Res 55:17–23.

Davis S, Aldrich TH, Stahl N, Pan L, Taga T, Kishimoto T, Ip NY, Yancopoulos GD (1993) LIFR beta and gp130 as heterodimerizing signal transducers of the tripartite CNTF receptor. Science 260:1805–1808.

Di Polo A, Cheng L, Bray GM, Aguayo AJ (2000) Colocalization of TrkB and brain-derived neurotrophic factor proteins in green-red-sensitive cone outer segments. Invest Ophthalmol Vis Sci 41:4014–4021.

Dow JK, deVere White RW (2000) Fibroblast growth factor 2: its structure and property, paracrine function, tumor angiogenesis, and prostate-related mitogenic and oncogenic functions. Urology 55:800–806.

Faff L, Nolte C (2000) Extracellular acidification decreases the basal motility of cultured mouse microglia via the rearrangement of the actin cytoskeleton. Brain Res 853:22–31.

Faktorovich EG, Steinberg RH, Yasumura D, Matthes MT, LaVail MM (1990) Photoreceptor degeneration in inherited retinal dystrophy delayed by basic fibroblast growth factor. Nature 347:83–86.

Faktorovich EG, Steinberg RH, Yasumura D, Matthes MT, LaVail MM (1992) Basic fibroblast growth factor and local injury protect photoreceptors from light damage in the rat. J Neurosci 12:3554–3567.

Florkiewicz RZ, Majack RA, Buechler RD, Florkiewicz E (1995) Quantitative export of FGF-2 occurs through an alternative, energy-dependent, non-ER/Golgi pathway. J Cell Physiol 162:388–399.

Fontaine V, Kinkl N, Sahel J, Dreyfus H, Hicks D (1998) Survival of purified rat photoreceptors *in vitro* is stimulated directly by fibroblast growth factor-2. J Neurosci 18:9662–9672.

Frade JM, Barde Y-A (1998) Microglia-derived nerve growth factor causes cell death in the developing retina. Neuron 20:35–41.

Frade JM, Rodriguez-Tebar A, Barde Y-A (1996) Induction of cell death by endogenous nerve growth factor through its p75 receptor. Nature 383:166–168.

Frasson M, Picaud S, Leveillard T, Simonutti M, Mohand-Said S, Dreyfus H, Hicks D, Sabel J (1999) Glial cell line-derived neurotrophic factor induces histologic and functional protection of rod photoreceptors in the *rd/rd* mouse. Invest Ophthalmol Vis Sci 40:2724–2734.

Gao H, Qiao X, Hefti F, Hollyfield JG, Knusel B (1997) Elevated mRNA expression of brain-derived neurotrophic factor in retinal ganglion cell layer after optic nerve injury. Invest Ophthalmol Vis Sci 38:1840–1847.

Goureau O, Hicks D, Courtois Y, de Kozak Y (1994) Induction and regulation of nitric oxide synthase in retinal Müller glial cells. J Neurochem 63:310–317.

Graeber MB, Streit WJ, Kiefer R, Schoen SW, Kreutzberg GW (1990) New expression of myelomonocytic antigens by microglia and perivascular cells following lethal motor neuron injury. J Neuroimmunol 27:121–132.

Graeber MB, Lopez-Redondo F, Ikoma E, Ishikawa M, Imai Y, Nakajima K, Kreutzberg GW, Kohsaka S (1998) The microglia/macrophage response in the neonatal rat facial nucleus following axotomy. Brain Res 813:241–253.

Harada T, Imaki J, Hagiwara M, Ohki K, Takamura M, Ohashi T, Matsuda H, Yoshida K (1995) Phosphorylation of CREB in rat retinal cells after focal retinal injury. Exp Eye Res 61:769–772.

Harada T, Imaki J, Ohki K, Ono K, Ohashi T, Matsuda H, Yoshida K (1996) Cone-associated *c-fos* gene expression in the light-damaged rat retina. Invest Ophthalmol Vis Sci 37:1250–1255.

Harada T, Harada C, Sekiguchi M, Wada K (1998a) Light-induced retinal degeneration suppresses developmental progression of flip-to-flop alternative splicing in GluR1. J Neurosci 18:3336–3343.

Harada T, Harada C, Watanabe M, Inoue Y, Sakagawa T, Nakayama N, Sasaki S, Okuyama S, Watase K, Wada K, Tanaka K (1998b) Functions of the two glutamate transporters GLAST and GLT-1 in the retina. Proc Natl Acad Sci USA 95:4663–4666.

Harada T, Harada C, Nakayama N, Okuyama S, Yoshida K, Kohsaka S, Matsuda H, Wada K (2000) Modification of glial-neuronal cell interactions prevents photoreceptor apoptosis during light-induced retinal degeneration. Neuron 26:533–541.

Harada T, Harada C, Mitamura Y, Akazawa C, Ohtsuka K, Ohno S, Takeuchi S, Wada K (2002) Neurotrophic factor receptors in epiretinal membranes after human diabetic retinopathy. Diabetes Care 25:1060–1065.

Heppner FL, Skutella T, Hailer NP, Haas D, Nitsch R (1998) Activated microglial cells migrate towards sites of excitotoxic neuronal injury inside organotypic hippocampal slice cultures. Eur J Neurosci 10:3284–3290.

Hesselgesser J, Horuk R (1999) Chemokine and chemokine receptor expression in the central nervous system. J Neurovirol 5:13–26.

Hicks D, Courtois Y (1990) The growth and behaviour of rat retinal Müller cells in vitro. 1. An improved method for isolation and culture. Exp Eye Res 51:119–129.

Ip NY, McClain J, Barrezueta NX, Aldrich TH, Pan L, Li Y, Wiegand SJ, Friedman B, Davis S, Yancopoulos GD (1993) The alpha component of the CNTF receptor is required for signaling and defines potential CNTF targets in the adult and during development. Neuron 10:89–102.

Ito D, Imai Y, Ohsawa K, Nakajima K, Fukuuchi Y, Kohsaka S (1998) Microglia-specific localisation of a novel calcium binding protein, Iba1. Mol Brain Res 57:1–9.

Ito D, Tanaka K, Suzuki S, Dembo T, Fukuuchi Y (2001) Enhanced expression of Iba1, ionized calcium-binding adapter molecule 1, after transient focal cerebral ischemia in rat brain. Stroke 32:1208–1215.

Jelsma TN, Friedman HH, Berkelaar M, Bray GM, Aguayo AJ (1993) Different forms of the neurotrophin receptor trkB mRNA predominate in rat retina and optic nerve. J Neurobiol 24:1207–1214.

Jing S, Wen D, Yu Y, Holst PL, Luo Y, Fang M, Tamir R, Antonio L, Hu Z, Cupples R, Louis JC, Hu S, Altrock BW, Fox GM (1996) GDNF-induced activation of the ret protein tyrosine kinase is mediated by GDNFR-alpha, a novel receptor for GDNF. Cell 85:1113–1124.

Jomary C, Thomas M, Grist J, Milbrandt J, Neal MJ, Jones SE (1999) Expression patterns of neurturin and its receptor components in developing and degenerative mouse retina. Invest Ophthalmol Vis Sci 40:568–574.

Ju WK, Lee MY, Hofmann HD, Kirsch M, Chun MH (1999) Expression of CNTF in Müller cells of the rat retina after pressure-induced ischemia. NeuroReport 10:419–422.

Kirsch M, Lee MY, Meyer V, Wiese A, Hofmann HD (1997) Evidence for multiple, local functions of ciliary neurotrophic factor (CNTF) in retinal development: expression of CNTF and its receptors and in vitro effects on target cells. J Neurochem 68:979–990.

Kiselev A, Socolich M, Vinos J, Hardy RW, Zuker CS, Ranganathan R (2000) A molecular pathway for light-dependent photoreceptor apoptosis in *Drosophila*. Neuron 28:139–152.

Klionsky DJ, Cueva R, Yaver DS (1992) Aminopeptidase I of *Saccharomyces cerevisiae* is localized to the vacuole independent of the secretory pathway. J Cell Biol 119:287–299.

Kreutzberg GW (1996) Microglia: a sensor for pathological events in the CNS. Trends Neurosci 19:312–318.

Kurokawa T, Sasada R, Iwane M, Igarashi K (1987) Cloning and expression of cDNA encoding human basic fibroblast growth factor. FEBS Lett 213:189–194.

LaVail MM, Unoki K, Yasumura D, Matthes MT, Yancopoulos GD, Steinberg RH (1992) Multiple growth factors, cytokines, and neuro-

trophins rescue photoreceptors from the damaging effects of constant light. Proc Natl Acad Sci USA 89:11249–11253.
LaVail MM, Yasumura D, Matthes MT, Lau-Villacorta C, Unoki K, Sung CH, Steinberg RH (1998) Protection of mouse photoreceptors by survival factors in retinal degenerations. Invest Ophthalmol Vis Sci 39:592–602.
Le WD, Rowe D, Xie W, Ortiz I, He Y, Appel SH (2001) Microglial activation and dopaminergic cell injury: an *in vitro* model relevant to Parkinson's disease. J Neurosci 21:8447–8455.
Maciejewski-Lenoir D, Chen S, Feng L, Maki R, Bacon KB (1999) Characterization of fractalkine in rat brain cells: migratory and activation signals for CX3CR-1-expressing microglia. J Immunol 163:1628–1635.
Marin-Teva JL, Almendros A, Calvente R, Cuadros MA, Navascues J (1998) Tangential migration of ameboid microglia in the developing quail retina: mechanism of migration and migratory behavior. Glia 22:31–52.
McGeer PL, McGeer ED (1998) Glial cell reactions in neurodegenerative diseases: pathophysiology and therapeutic interventions. Alzheimer Dis Assoc Disord 12[Suppl 2]:S1–6.
Mignatti P, Morimoto T, Rifkin DB (1992) Basic fibroblast growth factor, a protein devoid of secretory signal sequence, is released by cells via a pathway independent of the endoplasmic reticulum-Golgi complex. J Cell Physiol 151:81–93.
Nakajima K, Kohsaka S (2001) Microglia: activation and their significance in the central nervous system. J Biochem (Tokyo) 130:169–175.
Nakajima K, Kikuchi Y, Ikoma E, Honda S, Ishikawa M, Liu Y, Kohsaka S (1998) Neurotrophins regulate the function of cultured microglia. Glia 24:272–289.
Noell WK (1980) Possible mechanism of photoreceptor damage by light in mammalian eyes. Vision Res 20:1163–1171.
Nolte C, Kirchhoff F, Kettenmann H (1997) Epidermal growth factor is a motility factor for microglial cells in vitro: evidence for EGF receptor expression. Eur J Neurosci 9:1690–1698.
Papermaster DS, Windle J (1995) Death at an early age. Apoptosis in inherited retinal degenerations. Invest Ophthalmol Vis Sci 36:977–983.
Perez MT, Caminos E (1995) Expression of brain-derived neurotrophic factor and of its functional receptor in neonatal and adult rat retina. Neurosci Lett 183:96–99.
Piotrowicz RS, Martin JL, Dillman WH, Levin EG (1997) The 27-kDa heat shock protein facilitates basic fibroblast growth factor release from endothelial cells. J Biol Chem 272:7042–7047.
Portera-Cailliau C, Sung C-H, Nathans J, Adler R (1994) Apoptotic photoreceptor cell death in mouse models of retinitis pigmentosa. Proc Natl Acad Sci USA 91:3273–3281.
Reme CE, Grimm C, Hafezi F, Marti A, Wenzel A (1998) Apoptotic cell death in retinal degenerations. Prog Retin Eye Res 17:443–464.
Rohrer B, Korenbrot JI, LaVail MM, Reichardt LF, Xu B (1999) Role of neurotrophin receptor TrkB in the maturation of rod photoreceptors and establishment of synaptic transmission to the inner retina. J Neurosci 19:8919–8930.
Roque RS, Caldwell RB (1993) Isolation and culture of retinal microglia. Exp Eye Res 12:285–290.
Roque RS, Imperial CJ, Caldwell RB (1996) Microglial cells invade the outer retina as photoreceptors degenerate in Royal College of Surgeons rats. Invest Ophthalmol Vis Sci 37:196–203.
Sato Y, Rifkin DB (1988) Autocrine activities of basic fibroblast growth factor: regulation of endothelial cell movement, plasminogen activator synthesis, and DNA synthesis. J Cell Biol 107:1199–1205.
Shimojo M, Nakajima K, Takei N, Hamanoue M, Kohsaka S (1991) Production of basic fibroblast growth factor in cultured rat brain microglia. Neurosci Lett 123:229–231.
Slepko N, Levi G (1996) Progressive activation of adult microglial cells in vitro. Glia 16:241–246.
Steele F, O'Tousa JE (1990) Rhodopsin activation causes retinal degeneration in *Drosophila rdgC* mutant. Neuron 4:883–890.
Stoll G, Jander S (1999) The role of microglia and macrophages in the pathophysiology of the CNS. Prog Neurobiol 58:233–247.
Suzuki A, Nomura S, Morii E, Fukuda Y, Kosaka J (1998) Localization of mRNAs for trkB isoforms and p75 in rat retinal ganglion cells. J Neurosci Res 54:27–37.
Thanos S (1992) Sick photoreceptors attract activated microglia from the ganglion cell layer: a model to study the inflammatory cascades in rats with inherited retinal dystrophy. Brain Res 588:21–28.
Travis GH (1998) Mechanisms of cell death in the inherited retinal degenerations. Am J Hum Genet 62:503–508.
Ugolini G, Cremisi F, Maffei L (1995) Trk A, Trk B and p75 mRNA expression is developmentally regulated in the rat retina. Brain Res 704:121–124.
von Bartheld CS (1998) Neurotrophins in the developing and regenerating visual system. Histol Histopathol 13:437–459.
von Heijne G (1983) Patterns of amino acids near signal-sequence cleavage sites. Eur J Biochem 133:17–21.
Wahlin KJ, Campochiaro PA, Zack DJ, Adler R (2000) Neurotrophic factors cause activation of intracellular signaling pathways in Müller cells and other cells of the inner retina, but not photoreceptors. Invest Ophthalmol Vis Sci 41:927–936.
Wen R, Song Y, Cheng T, Matthes MT, Yasumura D, LaVail MM, Steinberg RH (1995) Injury-induced upregulation of bFGF and CNTF mRNAs in the rat retina. J Neurosci 15:7377–7385.
Wen R, Cheng T, Song Y, Matthes MT, Yasumura D, LaVail MM, Steinberg RH (1998) Continuous exposure to bright light upregulates bFGF and CNTF expression in the rat retina. Curr Eye Res 17:494–500.
Weskamp G, Reichardt LF (1991) Evidence that biological activity of NGF is mediated through a novel subclass of high affinity receptors. Neuron 6:649–663.
Yano H, Chao MV (2000) Neurotrophin receptor structure and interactions. Pharmacol Acta Helv 74:253–260.
Yoshida K, Muraki Y, Ohki K, Harada T, Ohashi T, Matsuda H, Imaki J (1995) C-fos gene expression in rat retinal cells after focal retinal injury. Invest Ophthalmol Vis Sci 36:251–254.
Zack DJ (2000) Neurotrophic rescue of photoreceptors: are Müller cells the mediators of survival? Neuron 26:285–286.

ACADEMIC PRESS

Biochemical and Biophysical Research Communications 295 (2002) 651–656

BBRC

www.academicpress.com

The Ras-like small GTP-binding protein Rin is activated by growth factor stimulation☆

Mitsunobu Hoshino[a,b,*] and Shun Nakamura[a]

[a] *Division of Biochemistry and Cellular Biology, National Institute of Neuroscience, National Center of Neurology and Psychiatry (NCNP), 4-1-1, Ogawahigashi, Kodaira, Tokyo 187-8502, Japan*

[b] *Department of Radiation Oncology, Graduate School of Medicine, The University of Tokyo, 7-3-1, Hongo, Bunkyo, Tokyo 113-0033, Japan*

Received 17 June 2002.

Abstract

A novel 25 K Ras-like protein, Rin, binds calmodulin in a Ca^{2+}-dependent manner and is considered to participate in a calcium/calmodulin-mediated signaling pathway. However, little is known about Rin signaling mechanism. Here we examined the signal transduction pathway through Rin protein using pull down assay system. When we stimulated Rin-expressed Cos-7 cells with ionomycin, phorbol 12-myristate 13-acetate or epidermal growth factor (EGF), Rin protein was rapidly activated. Moreover, cells cotransfected with Rin and mSos showed a similar Rin activation profile, and Rin protein was coimmunoprecipitated with mSos protein in vivo. When cells were cotransfected with Rin and Ras-GTPase-activating proteins, basal Rin activity was decreased. Association with Rin and calmodulin was potentiated after stimulation and Rin activation was regulated by both calcium ion and calmodulin. These studies suggest that Rin may be involved in EGF receptor and mSos-mediated signaling pathway and may participate in calcium/calmodulin-mediated cellular processes.

Keywords: Ras; Rin; Calcium; Calmodulin; Sos; EGF; GTP-binding protein; GTPase-activating protein (GAP)

Small guanine nucleotide-binding proteins of the Ras superfamily serve as key regulators in the intracellular signaling processes, such as cell proliferation, differentiation, and survival of various types of cells [1–3]. Ras regulates molecular events by recycling between inactive GDP-bound state and active GTP-bound state. Guanine nucleotide exchange factors, such as mSos, catalyze the dissociation of Ras-bound GDP and the binding of GTP. Inactivation of Ras occurs through Ras-GTPase-activating proteins (RasGAPs) by accelerating the intrinsic Ras-GTPase activity. When cells are stimulated by several growth factors, Ras transduces signals triggered by growth factor stimulation to downstream effectors, including Raf, Ral guanine nucleotide dissociation stimulator (RalGDS) family, and phosphatidylinositol-3 kinase and induces many cellular responses.

Rin is a novel 25 K Ras-like protein (218 a.a.) isolated from mouse retina, and binds GTP in vitro [4,5]. Rin has a high identity with Ras effector domain sequences but lacks a C-terminal CAAX motif [4,6]. In general, CAAX-motif-containing protein is posttranslationally modified by isoprenyl group and is targeted to the plasma membrane [6]. In spite of lacking CAAX-motif, Rin protein is membrane-localized similar to Ras [4]. Rin is expressed only in neuron and brain [4], and binds calmodulin in a Ca^{2+}-dependent manner through a C-terminal binding motif [4], indicating that Rin might be involved in calcium-mediated signaling process in neuronal cells. However, little is known about Rin protein and its signaling mechanisms have not yet been elucidated.

In this study, we investigated the molecular signal transduction mechanism of Rin protein. We developed a

☆ *Abbreviations:* BAPTA/AM, 1,2-bis(*O*-aminophenoxy)ethane-*N*,*N*,*N*′,*N*′-tetraacetic acid acetoxymethyl ester; EGF, epidermal growth factor; EDTA, ethylenediamine-*N*,*N*,*N*′,*N*′-tetraacetic acid; GAP, GTPase-activating proteins; GMPPNP, 5′-guanylylimidodiphosphate; GST, glutathione-*S*-transferase; HA, hemagglutinin; PBS, phosphate-buffered saline; PMSF, phenylmethanesulfonyl fluoride; RalGDS, Ral guanine nucleotide dissociation stimulator; RBD, Ras-binding domain; TPA, phorbol 12-myristate 13-acetate.

* Corresponding author.
E-mail address: hoshinom@ncnp.go.jp (M. Hoshino).

0006-291X/02/$ - see front matter
PII: S0006-291X(02)00731-3

pull down assay system that can estimate the activity of Rin protein and demonstrate that Rin protein is rapidly activated after calcium ionophore ionomycin, phorbor ester phorbol 12-myristate 13-acetate (TPA), or epidermal growth factor (EGF) stimulations in Cos-7 cells. Rin protein is also activated when cells are cotransfected with mSos cDNA and is coimmunoprecipitated with mSos protein. Rin activity is inhibited when cells are cotransfected with RasGAPs, not with Rap1GAP protein. Moreover, association of Rin protein with calmodulin is potentiated after stimulation and the stimulation-induced Rin activation is Ca^{2+}-dependent. The Rin deletion mutant protein that lacks calmodulin-binding domain binds an effector protein stimulation-independently and more tightly than full-length Rin protein does. The deletion mutant Rin protein shows higher affinity for mSos protein than the full-length Rin protein does. These studies suggest that Rin may play a pivotal role in growth factor receptor-mediated signal transduction mechanisms through mSos protein and may be involved in calcium/calmodulin-mediated signaling pathways.

Materials and methods

Expression plasmids. The mouse Rin expression constructs were produced by polymerase chain reaction amplification, in which mouse whole brain cDNAs were used as a template. The products were subcloned to the pEF-Bos mammalian expression vectors [7] with a hemagglutinin (HA)-tag or a Myc-tag. The constitutively active RinV29 mutant (Gly29 was substituted to Val) and the Rin deletion mutant (encoding 1–200 a.a. of Rin protein) were generated by PCR-based site-directed mutagenesis. The coding regions of all constructs were confirmed by DNA sequencing. A glutathione-*S*-transferase (GST)-fused RalGDS fusion construct encoding Ras-binding domain (RBD; [8]) was generated by inserting RalGDS RBD into pGEX vectors (Amersham Biosciences; Piscataway, NJ).

Antibodies and reagents. Anti-c-Myc 9E10 antibody, anti-Sos1 antibody, and anti-calmodulin I antibody were purchased from Santa Cruz (Santa Cruz, CA). An anti-HA high affinity antibody (3F10) was from Roche (Indianapolis, IN). Ionomycin, TPA, EGF, and calmodulin–agarose were purchased from Sigma (St. Louis, MO). BAPTA/AM was from Dojin (Kumamoto, Japan). Anti-Rin antibody, GDP, and a nonhydrolyzable GTP analog 5′-guanylylimidodiphosphate (GMPPNP) were from Calbiochem (La Jolla, CA).

Cell cultivation. Cos-7 cells were obtained from American Type Culture Collection (Rockville, MD) and were cultured in Dulbecco's modified Eagle's medium (Nissui, Tokyo) supplemented with 10% fetal bovine serum (Intergen, Purchase, NY), 2 mM L-glutamine, and penicillin/streptomycin and incubated at 37 °C in an atmosphere of 5% CO_2. Serum-starved cells were obtained by incubation for 24 h in the medium without fetal bovine serum.

Two-hybrid screening. A mouse whole brain library #ML4008AH (Clontech, Palo Alto, CA) was subjected to a two-hybrid screen, using mouse full-length RinV29 mutant as a bait. The Matchmaker Two-Hybrid System (Clontech) was used according to manufacturer's instruction. About 3.0×10^7 transformants were screened and yielded 88 positive colonies (H. Izumi and S. Hattori, NCNP, unpublished result).

Recombinant HA-Rin protein purification. Escherichia coli strain DH5α transformed with pGEX vector containing HA-tagged mouse Rin cDNA was induced with 0.1 mM isopropyl-β-D-thiogalactopyranoside (IPTG) and cultured overnight at 25 °C. After harvesting, bacterial pellets were lysed in a bacterial lysis buffer (20 mM Tris–HCl (pH 8.0), 100 mM NaCl, 2.5 mM $MgCl_2$, 10% glycerol, 0.1% Nonidet P40, 10 mM 2-mercaptoethanol, 1 mM *O,O′*-bis(2-aminoethyl)ethyleneglycol-*N,N,N′,N′*-tetraacetic acid (EGTA), 20 μg/ml DNase I, 0.1 mM phenylmethanesulfonyl fluoride (PMSF), 10 μg/ml of aprotinin, antipain, and leupeptin) and sonicated for 5 min. Lysates were then centrifuged at 13,000*g* at 4 °C for 20 min and supernatants were purified with glutathione (GSH)–Sepharose beads (Amersham). Bound GST-fused HA-Rin protein was eluted with 10 mM glutathione and digested with thrombin for GST-tag cleavage. Purified HA-Rin protein was concentrated to 2 mg/ml and kept frozen at −80 °C before use.

Transfection. Semi-confluent Cos-7 cells (2×10^6 cells in 60 mm dish) were transiently transfected with an expression vector by Lipofectamine 2000 (Invitrogen, Carlsbad, CA) employing the protocol provided by the manufacturer. Two days after transfection, transfectants were washed once with phosphate-buffered saline (PBS) buffer and lysed for several assays.

Pull down assay. Cos-7 cells were washed once with an ice-cold PBS buffer and lysed in a lysis buffer (50 mM Tris–HCl (pH 7.5), 150 mM NaCl, 2.5 mM $MgCl_2$, 10% glycerol, 1% Nonidet P40, 10 mM NaF, 1 mM Na_3VO_4, 0.1 mM PMSF, 10 μg/ml aprotinin and leupeptin). Cell lysates were clarified by centrifugation at 13,000*g* at 4 °C for 20 min. Supernatants were incubated with GST-RalGDS RBD protein (10 μg) immobilized on glutathione–Sepharose beads at 4 °C for 2 h. The beads were washed twice with an lysis buffer. Beads and bound Rin proteins were suspended in 20 μl Laemmli sample buffer. Rin-GTP levels were analyzed by immunoblot analysis.

Immunoprecipitation. Each Cos-7 cell lysate (from 60 mm dish) was gently incubated with 1 μg antibody coupled with 20 μl of protein G–Sepharose beads (Amersham) at 4 °C for 2 h. Proteins bound to antibody–protein G beads were washed twice with an lysis buffer, eluted from the beads using Laemmli sample buffer, and were subjected to SDS–PAGE.

Western blot analysis. Protein samples were separated by SDS–PAGE, transferred to nitrocellulose membrane (Schleicher and Schuell, Dassel, Germany), and probed with a primary antibody at 1:1000 dilution in PBS containing 0.1% Tween 20 and 5% nonfat dry milk (Becton Dickinson, Sparks, MD). The primary antibody was visualized with horseradish peroxidase-conjugated secondary antibody (Amersham) at 1:10,000 dilution and chemiluminescence (Perkin–Elmer Life Sciences, Boston, MA).

Results and discussions

Rin activation after growth factor stimulation

At first, a yeast two-hybrid screening for proteins that interact with an active form of Rin was performed. Constitutively active Rin mutant RinV29 was used as a bait. The cognate V12 mutant in Ras was shown to have a reduced intrinsic GTPase activity and was regarded to as a constitutively active mutant [1]. After screening, 88 positive clones were obtained. Most encoded fragments were Ras-binding domain (RBD) of Ral GDS family, such as RalGDS [9], RGL [10], and RGL3/RPM [11,12], suggesting that they are putative effectors of Rin. So we have developed a pull down assay system to measure Rin activation. This system is based on the specific affinity of GTP-bound Rin for the RBD of RalGDS. Fig. 1A shows that GMPPNP (a nonhydrolyzable GTP

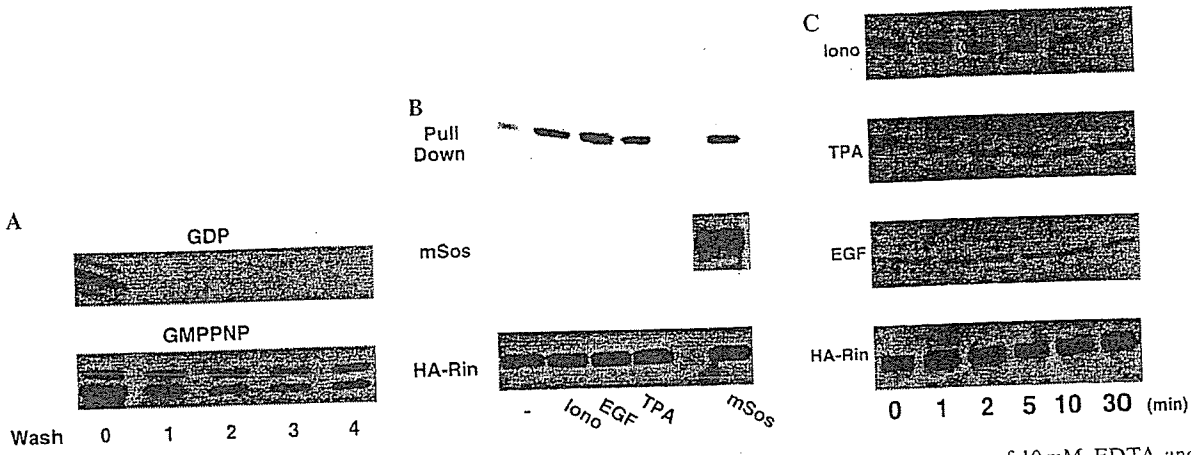

Fig. 1. Rin activation after stimulation. (A) Recombinant HA-Rin protein (0.5 μg) was incubated in the presence of 10 mM EDTA and 0.5 mM nucleotide (either GDP or GMPPNP) at 30 °C for 2.5 min in a total volume of 250 μl. Then $MgCl_2$ (final 20 mM) was added to the solution and incubated at 30 °C for 1 min, followed by pull down assay with glutathione-beads-immobilized GST-RalGDS RBD protein at 4 °C for 2 h. The beads were washed at indicated times and bound HA-Rin proteins were visualized by immunoblot analysis using an anti-HA antibody. (B) Cos-7 cells were transfected with HA-tagged pEF-Bos vector encoding Rin and mSos-encoding vector either alone or in pairs using Lipofectamine 2000. After 48 h, serum-depleted cells were stimulated with 0.5 μg/ml ionomycin, 0.1 μg/ml TPA, or 0.05 μg/ml EGF for 2 min. After cells were washed with an ice-cold PBS buffer, cells were lysed with an ice-cold lysis buffer. Cell lysates were cleared by centrifugation and HA-Rin proteins were pulled down with 10 μg of GST-RalGDS RBD protein, as described under Materials and methods. Data are representative of three independent experiments, which gave essentially identical results. (C) Cos-7 cells were transfected with pEF-Bos HA-Rin vector. After 48 h, serum-depleted cells were stimulated with 0.5 μg/ml ionomycin, 0.1 μg/ml TPA, or 0.05 μg/ml EGF for indicated periods (min) at 37 °C. The active HA-Rin proteins were isolated by pull down assay system and visualized as described under Materials and methods. Data are representative of three independent experiments, which gave essentially identical results.

analog)-bound Rin tightly binds to the GST-RalGDS RBD protein, and that GDP-bound Rin has no affinity for it. Rin protein binds to neither the glutathione beads alone nor GST proteins (data not shown). This pull down assay system was also effective when an anti-Rin antibody was used as a primary antibody (data not shown). Since GST-RalGDS RBD protein showed specificity for active Rin, we used this pull down assay system to investigate what kinds of stimulation do activate Rin protein in cultured cells. Rin protein was activated after calcium ionophore ionomycin, TPA, or EGF stimulation (Fig. 1B). The time-course of this ac-

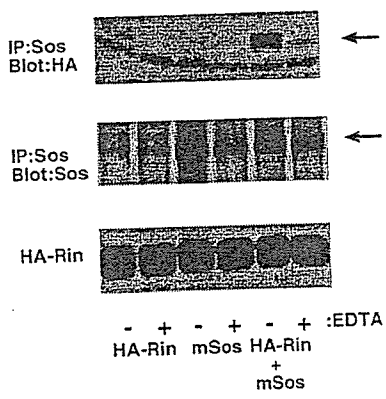

Fig. 2. mSos binds Rin. Cos-7 cells were transfected with pEF-Bos HA-Rin vector and mSos vector either alone or in pairs using Lipofectamine 2000. After 48 h, cells were lysed with an ice-cold lysis buffer or 10 mM EDTA-containing lysis buffer. Lysates were immunoprecipitated with an anti-Sos1 antibody and separated by SDS–PAGE, transferred to a membrane, and probed with an anti-HA antibody. The arrows in the first and second rows show coimmunoprecipitated HA-Rin proteins and immunoprecipitated mSos proteins, respectively. Data are representative of three independent experiments, which gave essentially identical results.

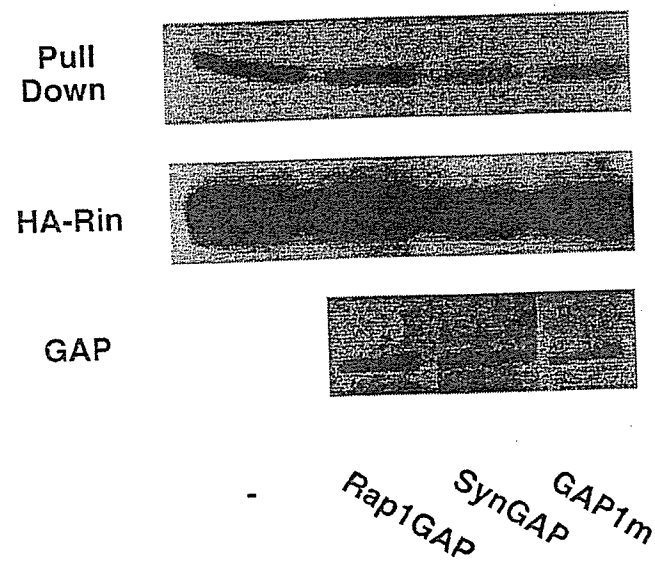

Fig. 3. GAP inhibits the activation of Rin. Cos-7 cells were cotransfected with pEF-Bos HA-Rin vector and each of pEF-Bos Myc-GAP vector using Lipofectamine 2000. After 48 h, serum-starved cells were lysed with an ice-cold lysis buffer and pulled down with GST-RalGDS RBD protein as described before. Data are representative of three independent experiments, which gave essentially identical results.

tivation was also examined (Fig. 1C). Ionomycin, TPA, or EGF stimulation induced a rapid increase in the amount of active Rin protein that was pulled down by GST-RalGDS RBD proteins. Ionomycin and EGF stimulations induced a transient activation of Rin, while TPA stimulation induced a persistent activation up to 30 min.

mSos directly binds to Rin

Many growth factor stimulations activate guanine nucleotide exchange factors, such as mSos, in the upstream of Ras. So we examined whether mSos protein could activate Rin protein. Fig. 1B shows that cotransfection of mSos and Rin vectors resulted in a constitutive activation of Rin protein. Next, we examined whether Rin directly binds to Sos, using a coimmunoprecipitation method. Fig. 2 shows that Rin protein was coimmunoprecipitated with mSos protein. Constitutively active mutant RinV29 could also be coimmunoprecipitated with mSos protein (data not shown). When EDTA was added to the cell lysate, Rin could no longer be coimmunoprecipitated with mSos protein (Fig. 2). These data suggest that growth factor stimulation in-

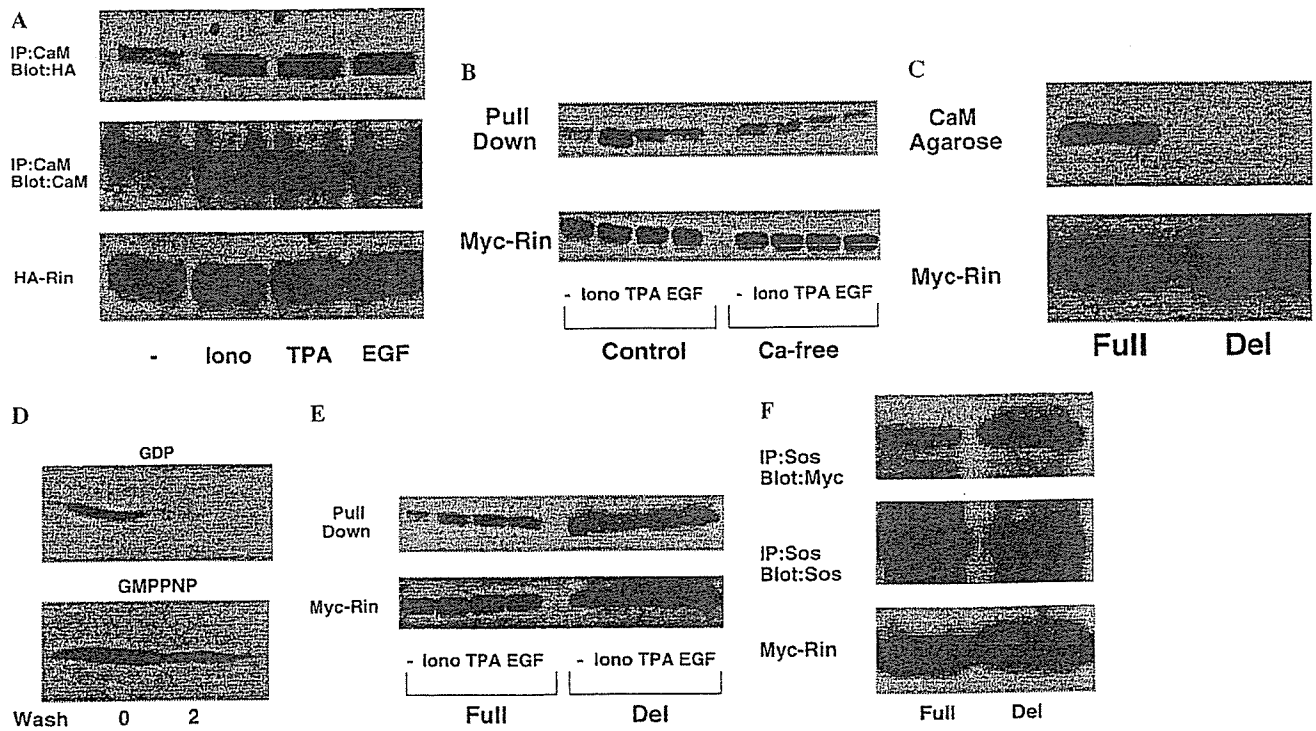

Fig. 4. Calcium/calmodulin involvement in Rin activation. (A) Cos-7 cells were transfected with pEF-Bos HA-Rin vector. After 48 h, serum-starved cells were stimulated with 0.5 μg/ml ionomycin, 0.1 μg/ml TPA, or 0.05 μg/ml EGF for 2 min, lysed and immunoprecipitated with an anti-calmodulin antibody. Immunoprecipitates were separated by SDS–PAGE, transferred to a membrane, and probed with an anti-HA antibody. Data are representative of three independent experiments, which gave essentially identical results. (B) Cos-7 cells were transfected with pEF-Bos HA-Rin vector. After 48 h, serum-starved cells were pretreated with 20 μM BAPTA/AM for 30 min and then stimulated with 0.5 μg/ml ionomycin, 0.1 μg/ml TPA or 0.05 μg/ml EGF for 2 min in the presence of 10 mM EDTA. After cells were washed with an ice-cold PBS buffer, cells were lysed with an ice-cold lysis buffer and the active HA-Rin proteins were isolated by pull down assay system and visualized as described under Materials and methods. Data are representative of three independent experiments, which gave essentially identical results. (C) Cos-7 cells were transfected with pEF-Bos full-length Myc-Rin vector or Myc-Rin deletion mutant (1–200 a.a.) vector. After 48 h, cells were lysed with an ice-cold lysis buffer, cleared by centrifugation and Myc-Rin proteins were pulled down with calmodulin-conjugated agarose beads (calmodulin-agarose) for 2 h at 4 °C. Pull down was performed as described. (D) Cos-7 cells were transfected with pEF-Bos Myc-Rin deletion mutant (1–200 a.a.) vector. After 48 h, cell lysates were collected and lysates were incubated in the presence of 10 mM EDTA and 0.5 mM nucleotide (either GDP or GMPPNP) at 30 °C for 2.5 min in a total volume of 250 μl. Then $MgCl_2$ (final 20 mM) was added to the solution and incubated at 30 °C for 1 min, followed by pulled down assay with glutathione-beads-immobilized GST-RalGDS RBD protein at 4 °C for 2 h. The beads were washed indicated times and bound Myc-Rin proteins were visualized by immunoblot analysis using an anti-Myc antibody. (E) Cos-7 cells were transfected with pEF-Bos full-length Myc-Rin vector or Myc-Rin deletion mutant (1–200 a.a.) vector. After 48 h, serum-starved cells were stimulated with 0.5 μg/ml ionomycin, 0.1 μg/ml TPA or 0.05 μg/ml EGF for 2 min at 37 °C. Cells were lysed with an ice-cold lysis buffer. Pull down assay was performed as described. Data are representative of three independent experiments, which gave essentially identical results. (F) Cos-7 cells were cotransfected with pEF-Bos full-length Myc-Rin vector and mSos vector, or Myc-Rin deletion mutant (1–200 a.a.) vector and mSos vector using Lipofectamine 2000. After 48 h, cells were lysed with an ice-cold lysis and lysates were immunoprecipitated with an anti-Sos1 antibody and separated by SDS–PAGE, transferred to a membrane, and probed with an anti-Myc antibody. Data are representative of three independent experiments, which gave essentially identical results.

duces the activation of Rin protein and that mSos protein directly associates with Rin protein. The mSos protein may be considered to be involved in the Rin activation pathway.

GAP inhibits Rin activation

GAP proteins function to inhibit the activity of low molecular weight G proteins by stimulating their intrinsic GTPase activity. We examined whether GAP proteins could inhibit Rin activation by pull down assay. Fig. 3 shows that both SynGAP [13] and GAP1^m [14], which are shown to be Ras-specific GAP proteins, inhibited Rin basal activity. On the other hand, Rap1-GAP, which is specific for Rap1 [15], not for Ras, could not inhibit Rin activation (Fig. 3). These data suggest that Ras-specific GAP protein may inhibit Rin activation.

Calmodulin involvement in Rin activation

Rin is a calmodulin-binding protein and might be involved in calcium-mediated signaling processes [4]. Then we raise a possibility that association of Rin and calmodulin might be potentiated after growth factor stimulations. We investigated this possibility by coimmunoprecipitation method. The amount of Rin–calmodulin complex was rapidly increased after growth factor stimulations (Fig. 4A). When Rin-transfected cells were pretreated with EDTA and BAPTA/AM, a membrane-permeable intracellular calcium ion chelator, growth factor-elicited Rin activation was significantly inhibited (Fig. 4B). These results suggest that ionomycin and TPA as well as EGF may activate Rin protein in a Ca^{2+}-dependent manner and that calcium ion and calmodulin may play an important role in the Rin-activation signaling pathway.

To further investigate the involvement of calmodulin in the cellular mechanisms that lead to the Rin activation, the deletion mutant of Rin protein (1–200 a.a.) was constructed. The coding region of this Rin deletion mutant was truncated at 200 a.a. and it could no longer bind calmodulin (Fig. 4C). Not the GDP-bound but the GMPPNP-bound deletion mutant of Rin protein could bind to the GST-RalGDS RBD protein (Fig. 4D). Thus, like the full-length Rin protein, the deletion mutant of Rin protein also binds to GST-RalGDS RBD protein GTP-dependently. This deletion mutant bound GST-RalGDS RBD protein stimulation-independently and the amount of the GTP-bound form seemed to be increased compared with the full-length Rin protein (Fig. 4E). We then considered a possibility that the stimulation-independent activation of the deletion mutant Rin protein was attributed to its higher affinity for mSos protein than the affinity of full-length Rin protein. To confirm this notion, the full-length and the deletion mutant Rin protein were coimmunoprecipitated with mSos protein. Fig. 4F shows that an anti-Sos1 antibody coimmunoprecipitated more amount of the deletion mutant protein than the full-length Rin protein.

These results suggest that calcium ion and calmodulin may be involved in the Rin-mediated signaling pathway and that calmodulin may regulate Rin activation.

In conclusion, Rin may function in EGF-receptor and mSos-dependent signaling pathway and may be involved in calcium-mediated cellular processes. Calmodulin can bind to Rin and may regulate the Rin activation pathway and Rin-mediated cellular events. To fully understand the molecular signal transduction mechanism, an effector of Rin and signaling cascade remains to be clarified and must be identified. The downstream signaling cascade of Rin is currently under investigation.

Acknowledgments

We thank Dr. N. Iida (NCNP) for valuable discussions and Drs. N. Suzuki, Y. Matsumoto, and T. Shimizu (University of Tokyo) for comments and continuous encouragement. We also thank Ms. H. Izumi (NCNP) for skillful technical assistance. M.H. is a research fellow of the Japan Society for the Promotion of Science.

References

[1] A.B. Vojtek, C.J. Der, Increasing complexity of the Ras signaling pathway, J. Biol. Chem. 273 (1998) 19925–19928.
[2] J.L. Bos, All in the family? New insights and questions regarding interconnectivity of Ras, Rap1, and Ral, EMBO J. 17 (1988) 6776–6782.
[3] N. Iida, K. Namikawa, H. Kiyama, H. Ueno, S. Nakamura, S. Hattori, Requirement of Ras for the activation of mitogen-activated protein kinase by calcium influx, cAMP, and neurotropin in hippocampal neurons, J. Neurosci. 21 (2001) 6459–6466.
[4] C.-H.J. Lee, N.G. Della, C.E. Chew, D.J. Zack, Rin, a neuron-specific and calmodulin-binding small G-protein, and Rit define a novel subfamily of Ras proteins, J. Neurosci. 16 (1996) 6784–6794.
[5] H. Shao, K. Kadono-Okuda, B.S. Finlin, D.A. Andres, Biochemical characterization of the Ras-related GTPases Rit and Rin, Arch. Biochem. Biophys. 371 (1999) 207–219.
[6] G.W. Reuther, C.J. Der, The Ras branch of small GTPases: Ras family members don't fall far from the tree, Curr. Opin. Cell Biol. 12 (2000) 157–165.
[7] S. Mizushima, S. Nagata, pEF-BOS, a powerful mammalian expression vector, Nucleic Acids Res. 18 (1990) 5322.
[8] B. Franke, J.-W.N. Akkerman, J.L. Bos, Rapid Ca^{2+}-mediated activation of Rap1 in human platelets, EMBO J. 16 (1997) 252–259.
[9] C.F. Albright, B.W. Giddings, J. Liu, M. Vito, R.A. Weinberg, Characterization of a guanine nucleotide dissociation stimulator for a ras-related GTPase, EMBO J. 12 (1993) 339–347.
[10] A. Kikuchi, S.D. Demo, Z.-H. Ye, Y.-W. Chen, L.T. Williams, ralGDS family members interact with the effector loop of ras p21, Mol. Cell. Biol. 14 (1994) 7483–7491.

[11] H. Shao, D.A. Andres, A novel RalGEF-like protein, RGL3, as a candidate effector for Rit and Ras, J. Biol. Chem. 275 (2000) 26914–26924.
[12] G.R.A. Ehrhardt, C. Korherr, J.S. Wieler, M. Knaus, J.W. Schrader, A novel potential effector of M-Ras and p21 Ras negatively regulates p21 Ras-mediated gene induction and cell growth, Oncogene 20 (2001) 188–197.
[13] J.H. Kim, D. Liao, L.F. Lau, R.L. Huganir, SynGAP: a synaptic RasGAP that associates with the PSD-95/SAP90 protein family, Neuron 20 (1998) 683–691.
[14] M. Maekawa, S. Li, A. Iwamatsu, T. Morishita, K. Yokota, Y. Imai, S. Kohsaka, S. Nakamura, S. Hattori, A novel mammalian Ras GTPase-activating protein which has phospholipid-binding and Btk homology regions, Mol. Cell. Biol. 14 (1994) 6879–6885.
[15] B. Rubinfeld, S. Munemitsu, R. Clark, L. Conroy, K. Watt, W.J. Crosier, F. McCormick, P. Polakis, Molecular cloning of a GTPase activating protein specific for the Krev-1 protein p21rap1, Cell 65 (1991) 1033–1042.

THE JOURNAL OF BIOLOGICAL CHEMISTRY
Vol. 277, No. 22, Issue of May 31, pp. 20026–20032, 2002
Printed in U.S.A.

Macrophage/Microglia-specific Protein Iba1 Enhances Membrane Ruffling and Rac Activation via Phospholipase C-γ-dependent Pathway*

Received for publication, September 24, 2001, and in revised form, March 22, 2002
Published, JBC Papers in Press, March 26, 2002, DOI 10.1074/jbc.M109218200

Hiroko Kanazawa, Keiko Ohsawa, Yo Sasaki, Shinichi Kohsaka‡, and Yoshinori Imai

From the Department of Neurochemistry, National Institute of Neuroscience, 4-1-1 Ogawahigashi, Kodaira, Tokyo 187-8502, Japan

Iba1 is a macrophage/microglia-specific calcium-binding protein that is involved in RacGTPase-dependent membrane ruffling and phagocytosis. In this study, we introduced Iba1 into Swiss 3T3 fibroblasts and demonstrated the enhancement of platelet-derived growth factor (PDGF)-induced membrane ruffling and chemotaxis. Wortmannin treatment did not completely suppressed this enhanced membrane ruffling in Iba1-expressing cells, whereas it did in Iba1-nonexpressing cells, suggesting that the enhancement is mediated through a phosphatidylinositol 3-kinase (PI3K)-independent signaling pathway. Porcine aorta endothelial cells transfected with expression constructs of Iba1 and PDGF receptor add-back mutants were used to analyze the signaling pathway responsible for the Iba1-induced enhancement of membrane ruffling. In the absence of Iba1 expression, PDGF did not induced membrane ruffling in cells expressing the Tyr-1021 receptor mutant, which is capable of activating phospholipase C-γ (PLC-γ) but not PI3K. In contrast, in the presence of Iba1 expression, membrane ruffling was formed in cells expressing the Tyr-1021 mutant. In addition, Rac was shown to be activated during membrane ruffling in cells expressing Iba1 and the Tyr-1021 mutant. Furthermore, dominant negative forms of PLC-γ completely suppressed PDGF-induced Iba1-dependent membrane ruffling and Rac activation. These results indicate the existence of a novel signaling pathway where PLC-γ activates Rac in a manner dependent on Iba1.

Cell motility is a dynamic process driven by structurally and functionally coordinated reorganization of the actin cytoskeleton (1, 2). Among various types of cells, macrophages are extremely motile to migrate rapidly to sites of infection or inflammation, suggesting that highly integrated systems should exist to regulate the actin cytoskeleton in macrophages (3, 4). In addition to circulating monocytes/macrophages, there are many types of tissue-resident macrophages, including Langerhans cells, Kupffer cells, dendritic cells, splenocytes, and microglia. In response to various pathological phenomena, microglia are activated to exhibit drastic changes in shape and the abilities to become locomotive and to phagocytose (5, 6). These cellular reactions are also profoundly underlaid by dynamic remodeling of the actin cytoskeleton.

The Rho family GTPases, Cdc42, Rac, and Rho, are known to be molecular switches that organize remodeling of the actin cytoskeleton (7). Among them, in fibroblasts, Rac is activated by receptor tyrosine kinases such as platelet-derived growth factor receptor (PDGFR),[1] leading to the formation of lamellipodia and membrane ruffles (8). Dominant active RacV12 induces remarkable membrane ruffling, and dominant negative RacN17 completely inhibits peptide growth factor-induced membrane ruffling; therefore, Rac is recognized to be an essential component in this type of membrane ruffling (8). Some studies describe signaling molecules capable of interacting with Rac; however, the processes by which receptor tyrosine kinases activate Rac are not fully understood.

Previously, we identified a calcium-binding protein, Iba1, which is restrictedly expressed in macrophages/microglia (9), and showed that the expression of Iba1 is up-regulated in activated microglia following facial nerve axotomy (10). In our recent study, Iba1 was further characterized by using a microglial cell line MG5 (11) and loss of function Iba1 mutants, and it was demonstrated that mutant Iba1 effectively suppresses the membrane ruffling produced by stimulation with macrophage colony-stimulating factor (M-CSF) or by expression of dominant active RacV12 (12). These observations suggested that Iba1 was involved in the molecular basis of membrane ruffling of macrophages/microglia and interacted with the signaling of Rac, which is a key molecule in controlling membrane ruffling also in macrophages (13). Iba1 is therefore considered to be one of the candidate molecules underlying the extremely motile property of macrophages/microglia.

In this study, to address this hypothesis, we introduced Iba1 in Swiss 3T3 fibroblasts, porcine aorta endothelial (PAE) cells, and Chinese hamster ovary (CHO) cells, none of which expresses endogenous Iba1, and examined the formation of membrane ruffles, chemotaxis, and profiles of intracellular signaling molecules, including PDGFR, phosphatidylinositol-3 kinase (PI3K), phospholipase C-γ (PLC-γ), and Rac.

* This work was supported by the Organization for Pharmaceutical Safety and Research, by a grant from the Japanese Ministry of Health, Labour and Welfare, and by a grant-in-aid for scientific research on priority areas from the Japanese Ministry of Education, Science, Sports, Culture and Technology. The costs of publication of this article were defrayed in part by the payment of page charges. This article must therefore be hereby marked "*advertisement*" in accordance with 18 U.S.C. Section 1734 solely to indicate this fact.

‡ To whom correspondence should be addressed: Tel.: 81-42-346-1721; Fax: 81-42-346-1751; E-mail:kohsaka@ncnp.go.jp.

[1] The abbreviations used are: PDGFR, platelet-derived growth factor receptor; M-CSF, macrophage colony-stimulating factor; PAE, porcine aorta endothelial; CHO, Chinese hamster ovary; PI3K, phosphatidylinositol-3 kinase; PLC, phospholipase C; FCS, fetal bovine serum; WT, wild type; GST, glutathione *S*-transferase; DMEM, Dulbecco's modified Eagle's medium; HRP, horseradish peroxidase; LPA, lysophosphatidic acid; PBS, phosphate-buffered saline; BSA, bovine serum albumin; FITC, fluorescein isothiocyanate; PKC, protein kinase C; $[Ca^{2+}]_i$, intracellular calcium; PAK, p21-activated kinase.

EXPERIMENTAL PROCEDURES

Cell Culture and Transfection—Swiss 3T3 cells were maintained in Dulbecco's modified Eagle's medium (DMEM) supplemented with 10% fetal calf serum (FCS). Mouse *iba1* cDNA (9) was inserted into the tetracycline-regulated expression vector pTet-Splice (Invitrogen) to construct pTet-iba1. The cells were transfected with pTet-iba1, transactivator pTet-tTAK, and pSV2-neo by calcium phosphate coprecipitation, and stably transfected clones were isolated by selection with 400 μg/ml G418 (Invitrogen).

PAE cells (14), kindly provided by Dr. C.-H. Heldin (Ludwig Institute for Cancer Research, Sweden) and Dr. Koutaro Yokote (Chiba University, Japan) were cultured in Ham's F12 medium (Invitrogen) supplemented with 10% FCS. pLXSN plasmids carrying wild type (WT) and a series of mutant human β-PDGFRs (15) were kindly provided by Dr. A. Kazlauskas (Schepens Eye Research Institute, Harvard Medical School, Boston, MA). F5 mutant PDGFR, which was constructed by the substitution of phenylalanines for five tyrosine residues that are required for the binding of PI3K, RasGAP, SHP-2, and PLC-γ1, is unable to associate with any of these proteins. Add-back mutants of PDGFR were generated by restoring tyrosine residues at individual binding sites for each of the receptor-associated proteins (15). PAE cells were transfected with the tetracycline-regulated Iba1-expressing system and cloned as described above. Subsequently, Iba1-expressing cells were transfected with WT PDGFR or the add-back series of PDGFR mutants by the FuGENE6 transfection reagent (Roche Molecular Biochemicals, Germany) and selected by 5 μg/ml of blasticidin S (Funakoshi, Japan).

PAE transfectants were incubated in Ham's F12 containing 0.5% FCS for 8 h before microinjection of 0.6 μg/μl pFLAG-CMV2 carrying WT and Y771F/Y783F *plc-γ1* cDNAs, which were kindly provided by Dr. P.-G. Suh (16) (Pohang University of Science and Technology, Korea). Injected PAE cells were maintained for 3 h at 37 °C to induce protein expression. Expression plasmids for glutathione *S*-transferase (GST)-PLC-γ1–2SH2 and GST-PI3-K SH2 (N) (17) were kindly provided by Dr. T. Takenawa and Dr. K. Fukami (Institute of Medical Science, University of Tokyo, Japan). The purified GST fusion proteins were microinjected into the cytosol and incubated for 10 min at 37 °C. The cells were then stimulated with PDGF (50 ng/ml) for 5 min.

CHO cells were maintained in RPMI 1640/Ham's F12/DMEM (2:1:1) medium supplemented with 10% FCS. CHO cells were transiently transfected using LipofectAMINE Plus reagent (Invitrogen) with pLXSN carrying WT *PDGFR*, pFLAG-CMV2 carrying WT or mutant *plc-γ1*, and pEGFP-C1 (CLONTECH, Palo Alto, CA) carrying WT-*iba1* or mutant *iba1*-(1–115) (12).

A microglial cell line, MG5, was maintained as described previously (12).

Western Blotting—Cells were lysed in radioimmune precipitation buffer containing 20 mM Tris-HCl, pH 7.4, 150 mM NaCl, 10% glycerol, 5 mM EDTA, 1% Triton-X100, 1% sodium deoxycholate, 0.1% SDS, 1 mM phenylmethylsulfonyl fluoride, 20 μg/ml aprotinin, 20 μM leupeptin, 1 mM sodium vanadate, and 10 μM pepstatin. The lysate was clarified by centrifugation, normalized for protein concentration, and subjected to SDS-PAGE. Separated proteins were electrotransferred to an Immobilon (Millipore, MA) membrane, which was then blocked with 25 mM Tris-HCl, pH 7.5, containing 125 mM NaCl, 0.1% Tween 20, and 4% skim milk. The membrane was incubated with anti-Iba1 antibody (1 μg/ml) (12), then subsequently with a horseradish peroxidase (HRP)-conjugated anti-rabbit IgG antibody (1:1500 dilution) (Bio-Rad, CA), and visualized using an ECL Western blotting detection system (Amersham Biosciences, Inc., UK).

Phalloidin Staining and Immunocytochemistry—Swiss 3T3 or PAE transfectants (1×10^4) were plated on a 13-mm poly-D-lysine (Sigma Chemical Co., St. Louis, MO)-coated glass coverslip, cultured for 2 days, then serum-starved for 13 h in DMEM without FCS (Swiss 3T3) or in Ham's F12 with 0.5% FCS (PAE) in the presence or absence of 0.5 μg/ml tetracycline. The cells were stimulated with human PDGF-BB (UBI, NY), bradykinin (Sigma), or lysophosphatidic acid (LPA) (Sigma), then fixed for 60 min at room temperature with 3% paraformaldehyde in phosphate-buffered saline (PBS). The cells were treated for 5 min with PBS containing 1 mg/ml sodium borohydride, permeabilized for 20 min with PBS containing 0.1% Triton-X100, and blocked for 2 h with PBS containing 3% normal goat serum and 3% bovine serum albumin (BSA) (blocking buffer). The cells were incubated for 13 h at 4 °C in blocking buffer containing 8 μg/ml rabbit anti-Iba1 antibody, then washed with PBS and incubated for 2 h in blocking buffer containing 5 μg/ml fluorescein isothiocyanate (FITC)-conjugated goat anti-rabbit IgG antibody (BioSource, Camarillo, CA) and 6 units/ml Texas Red-conjugated phalloidin (Molecular Probes, Eugene, OR). The cells were then observed with fluorescence microscope AX70 (Olympus, Japan) or confocal laser scanning microscope CLSM2010 (Amersham Biosciences, Inc.).

Chemotaxis Assay—Cell migration was assayed by a modified Boyden chamber method (18) using a 96-well chemotaxis chamber (Neuro Probe, Cabin John, MD). The lower wells that were filled with 25 μl of DMEM containing 1% BSA and PDGF were overlaid with an 8-μm pore polycarbonate filter (Neuro Probe) pre-coated with 100 μg/ml type I collagen (Cohesion, Palo Alto, CA). Above the membrane, the upper wells were set and loaded with 50 μl of DMEM with 1% BSA containing 3×10^5 trypsin-dispersed cells per milliliter. The chamber was then incubated at 37 °C for 8 h. The cells on the upper side of the filter were scraped off, and the cells that had migrated to the lower side of the filter were fixed and stained in PBS containing 12% formaldehyde, 10% ethanol, and 0.05% crystal violet. Cell numbers were counted in four fields per well. Values are means of triplicate experiments.

Determination of Activated Rac—The PAK pull-down assay was performed mainly as described previously (12, 19). Cells (10^6) were lysed in 500 μl of Hepes-buffered saline (25 mM Hepes-NaOH, pH 7.3, 150 mM NaCl, 5 mM $MgCl_2$, 0.5 mM EGTA, 20 mM β-glycerophosphate, 0.5% Triton-X100, 4% glycerol, 10 mM NaF, 2 mM sodium vanadate, 5 mM phenylmethylsulfonyl fluoride, 10 μM leupeptin, 10 μM pepstatin, and 0.5 mM dithiothreitol). The lysates were cleared by centrifugation, incubated with GST-PAK fusion protein (12, 19) and glutathione-Sepharose 4B (Amersham Biosciences, Inc.) for 30 min at 4 °C, and subsequently washed in Hepes-buffered saline. Bound activated Rac was visualized by Western blotting with an anti-Rac1 antibody (0.5 μg/ml) and HRP-conjugated anti-mouse goat IgG (1:1500 dilution) using the ECL system.

Immunoprecipitation—Serum-starved quiescent PAE and M-CSF-starved MG5 cells were stimulated with 50 ng/ml PDGF and 100 ng/ml mouse M-CSF (R&D Systems, Minneapolis, MN), respectively. The cells were lysed in radioimmune precipitation buffer at 4 °C for 20 min. Insoluble material was removed by centrifugation, and the cell lysates were normalized for protein concentration before immunoprecipitation. The lysates were incubated with 1.7 μg/ml anti-PLC-γ1 (UBI) or anti-PLC-γ2 (Santa Cruz Biotechnology, Santa Cruz, CA) antibody and with protein G-Sepharose beads (Amersham Biosciences, Inc.). The precipitated proteins were then subjected to Western blotting with an anti-phosphotyrosine antibody, 4G10 (Seikagaku, Japan), and HRP-conjugated anti-mouse goat IgG (Amersham Biosciences, Inc.) using the ECL system.

RESULTS

Enhancement of PDGF-induced Membrane Ruffling in Iba1-expressing Swiss 3T3 Cells—In this study, to analyze the functions of intact Iba1, we transfected a tetracycline-inducible Iba1-expression construct into Swiss 3T3, a fibroblast cell line expressing no endogenous Iba1. As a result, we established five clones of stable transfectants exhibiting inducible Iba1 expression. Immunoblotting with the anti-Iba1 antibody demonstrated that the expression of Iba1 was tightly inhibited under the presence of tetracycline whereas 13 or 22 h after the removal of tetracycline, strong expression of Iba1 was induced (Fig. 1*A*).

In Swiss 3T3 cells, bradykinin, LPA, and PDGF are known to specifically activate Cdc42, Rho, and Rac, respectively, and lead the cells to form filopodia, stress fibers, and membrane ruffles (7). To examine the effects of Iba1 on these structures, the Iba1-inducible cells were serum-starved, stimulated with bradykinin, LPA, and PDGF, and stained with phalloidin to visualize the actin cytoskeleton. When Iba1 expression was suppressed in the presence of tetracycline, the cells formed filopodia, stress fibers, and membrane ruffles in response to bradykinin, LPA, and PDGF, respectively (Fig. 1*B*), as reported for parent Swiss 3T3 cells (8, 20–22). When Iba1 expression was induced by tetracycline removal, the cells also formed filopodia and stress fibers indistinguishable from those shown in the absence of Iba1 expression after stimulation with bradykinin and LPA (Fig. 1*B*). By contrast, in response to PDGF, the Iba1-expressing cells formed apparently enhanced membrane ruffles in comparison with the Iba1-nonexpressing cells (Fig. 1*B*). When the cells were doubly stained with phalloidin and the anti-Iba1 antibody after PDGF stimulation, Iba1 was

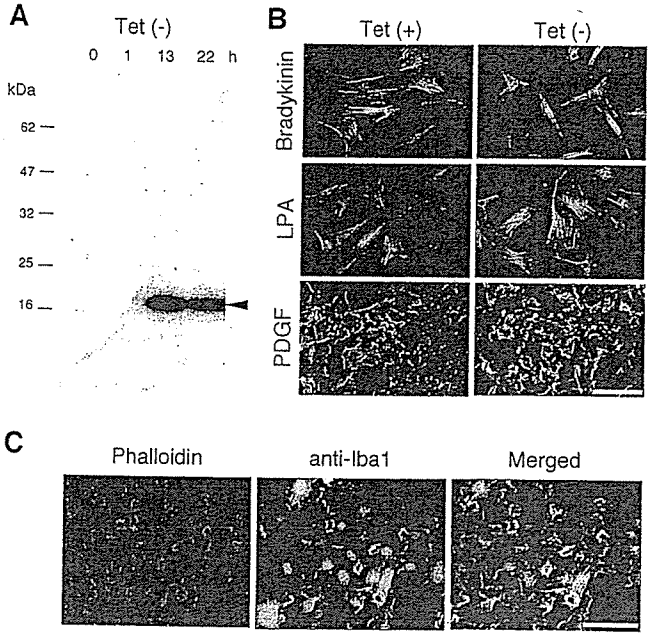

FIG. 1. **Enhanced membrane ruffling of Iba1-expressing Swiss 3T3 cells.** *A*, inducible expression of Iba1 in Swiss 3T3 transfectants. Swiss 3T3 transfectants, after tetracycline removal for indicated times, were lysed and subjected to Western blot analysis with anti-Iba1 antibody. The *arrowhead* indicates the position of Iba1. *B*, phalloidin staining of Swiss 3T3 transfectants. Serum-starved transfectants cultured in the presence or absence of tetracycline were stimulated with 100 ng/ml bradykinin, 100 ng/ml LPA, or 3 ng/ml PDGF for 10 min. The cells were then fixed and stained with Texas Red-conjugated phalloidin. *Scale bar*, 50 μm. *C*, double staining of Swiss 3T3 transfectants. Iba1-expressing Swiss 3T3 transfectants were stimulated with 3 ng/ml PDGF for 10 min. The cells were fixed and then doubly stained with Texas Red-phalloidin and anti-Iba1 antibody. *Scale bar*, 50 μm.

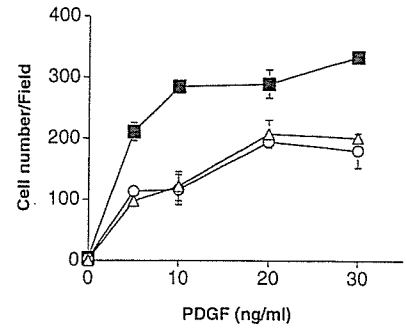

FIG. 2. **Enhanced chemotaxis of Iba1-expressing Swiss 3T3 cells.** Swiss 3T3 cells (*open triangles*) and Iba1-transfectans cultured in the presence (*open circles*) or absence (*closed squares*) of tetracycline were examined for chemotaxis against PDGF by Boyden chamber. Values are means of triplicate experiments.

shown to be localized at the sites of membrane ruffles, together with F-actin (Fig. 1*C*), but Iba1 did not colocalize with F-actin in filopodia or stress fibers induced by bradykinin or LPA stimulation (data not shown). All other clones of the transfectants exhibited similar enhanced membrane ruffling (data not shown), indicating that Iba1 definitely enhances PDGF-dependent membrane ruffling in Swiss 3T3 transfectants.

Enhanced Chemotaxis of Iba1-expressing Swiss 3T3 Cells—Because membrane ruffling is considered to be related to cell motility (23), we determined the chemotaxis of Iba1-expressing cells by the Boyden chamber method (18) using PDGF as a chemoattractant. As shown in Fig. 2, Swiss 3T3 parent cells and the Iba1-nonexpressing transfectants showed similar motile responses toward PDGF in a dose-dependent manner, whereas the Iba1-expressing cells exhibited about a 2-fold increase in chemotactic response. Similar results were obtained in all clones of Iba1 transfectants. Tetracycline itself had no effect on PDGF-induced migration in Swiss 3T3 cells (data not shown). These results indicate that Iba1 is also able to enhance the chemotaxis of Swiss 3T3 cells.

PI3K-independent Membrane Ruffling of Iba1-expressing Swiss 3T3 Cells—The PI3K signaling pathway is reported to be necessary for PDGF-induced membrane ruffling of Swiss 3T3 cells (24). To investigate whether this pathway is also required for the Iba1-dependent enhancement of membrane ruffling, the effect of PI3K inhibitors, wortmannin and LY294002, on PDGF-induced membrane ruffling was examined in both Iba1-nonexpressing and -expressing cells. Without treatment with the inhibitors, both transfectants formed membrane ruffles as a result of PDGF stimulation, but the extent of ruffle formation was greater in Iba1-expressing cells than in Iba1-nonexpressing cells (Fig. 3). With the wortmannin treatment, membrane ruffling of Iba1-nonexpressing transfectants was completely abolished, indicating that the formation of membrane ruffles of Iba1-nonexpressing Swiss 3T3 cells depends totally on the PI3K signaling pathway. By contrast, the Iba1-expressing cells formed obvious membrane ruffles even after wortmannin treatment, indicating that membrane ruffling of Iba1-expressing cells does depend on a certain signaling pathway in addition to PI3K. The same results were obtained using another PI3K inhibitor, LY294002 (Fig. 3). These observations led us to speculate that the enhanced membrane ruffling associated with Iba1 is transduced by a PI3K-independent pathway.

Involvement of PLC-γ in Membrane Ruffling of Iba1-expressing PAE Cells—To elucidate the possibility that Iba1 is involved in the PI3K-independent signaling pathway, we utilized the add-back mutants of PDGFR, which were transfected into PAE cells lacking endogenous PDGFR (14). PDGFR associates with various signaling molecules via its autophosphorylated tyrosines. PI3K selectively targets tyrosine at amino acid positions 740 (Tyr-740) and Tyr-751, whereas RasGAP, SHP-2, and PLC-γ recognize Tyr-771, Tyr-1009, and Tyr-1021, respectively. These signaling molecules are unable to bind to the PDGFR F5 mutant, in which all of the five tyrosines were replaced by phenylalanines (15). PAE cells, which did not express Iba1, were co-transfected with the Iba1-inducible construct and PDGFR mutant-expression vectors. Similar expression levels were seen for all the PDGFRs in the stable transfectants, as measured by fluorescence-activate cell sorting analysis (data not shown). Without stimulation with PDGF, the morphology of the cells was identical in the presence and absence of Iba1 expression (data not shown). When the Iba1-nonexpressing cells were stimulated with PDGF, obvious membrane ruffles were formed in the cells co-transfected with WT PDGFR receptor or Y740/51 mutant, which is capable of PI3K activation, in agreement with a previous report (25). In contrast, cells expressing F5 or Tyr-1021 receptor did not respond to PDGF (Fig. 4). These observations indicate the necessity of PI3K signaling for PDGF-induced membrane ruffling in the absence of Iba1. On the other hand, after the induction of Iba1, apparent membrane ruffles were formed in the cells transfected with Tyr-1021 mutant, capable of activation of PLC-γ. Membrane ruffling was also detected in the Iba1-expressing cells with the WT or Y740/51 mutant, as in the Iba1-nonexpressing cells (Fig. 4). Cells expressing Tyr-771, Tyr-1009, or kinase inactive receptor (Arg-635) did not show PDGF-induced membrane ruffling regardless of Iba1 expression (data not shown). These observations strongly suggest that PLC-γ is the key signaling molecule in Iba1-dependent and wortmannin-resistant membrane ruffling.